

Ningappa, A., & Suresha, S. N. (2020).
Laboratory evaluation of long-term aging
effect on linear viscoelastic and fatigue
properties of FAM mixtures. *Construction and
Building Materials*, 241

doi:10.1016/j.conbuildmat.2020.118087

<https://doi.org/10.1016/j.conbuildmat.2020.118087>

1 **Laboratory Evaluation of Long-Term Aging Effect**
2
3
4 **on Linear Viscoelastic and Fatigue Properties of**
5
6
7
8 **FAM Mixtures**
9

10
11
12
13 **A. Ningappa^{1*} and S. N. Suresha²**
14
15

16
17 ^{1*} Department of Civil Engineering, National Institute of Technology Karnataka, Surathkal,
18
19
20 India - 575025, E-mail: baningu.2010@gmail.com
21
22

23
24
25
26 ² Associate Professor, Department of Civil Engineering, National Institute of Technology
27
28
29 Karnataka, Surathkal, India - 575025, E-mail: sureshasn@nitk.edu.in
30
31

17 **ABSTRACT**

18 Aging is considered as one of the major factor which causes an increase in stiffness and
19 brittleness to asphaltic mixture. This study aimed at evaluating the effect of different aging
20 protocol on viscoelastic and fatigue properties of Fine Aggregate Matrix (FAM) which
21 represents the finer portion (passing 2.36 mm sieve size) of asphalt concrete mixtures. To
22 evaluate the effect of aging on viscoelastic and fatigue properties of FAM mixtures, six
23 different long-term aging levels (6 hrs at 135°C, 12 hrs at 135°C, 24 hrs at 135°C, 5 days at
24 95°C, and 12 days at 95°C aging on FAM loose mixture and 5 days at 85°C on compacted
25 FAM specimens) were considered. Linear Visco-Elastic (LVE) limit of each FAM mixtures
26 was initially determined by conducting strain sweep test. Viscoelastic properties ($|G^*|$ and δ)
27 and master curve shape parameters of FAM mixtures were further determined from
28 temperature and frequency sweep test. Fatigue properties of FAM mixtures at different aging
29 levels were evaluated using strain controlled time sweep test. Irrespective of the aging level
30 applied to the FAM specimen, the LVE limit was found almost constant for all FAM
31 mixtures. Viscoelastic properties ($|G^*|$ and δ) for FAM specimen aged for 24 hrs at 135°C,
32 and 12 days at 95°C aged FAM mixtures showed similar results from the master curve plots.
33 The fatigue properties of FAM mixtures decreased as the aging level changed from 5 days at
34 95°C to higher level aging of 12 days at 95°C. Despite of the similar viscoelastic properties,
35 the trend observed between FAM mixtures aged 12 days at 95°C and 24 hrs at 135°C were
36 not found to have similar fatigue properties. Findings of this study on FAM phase can be
37 successfully used to characterize the effect of long-term aging on performance studies of
38 FAM mixtures.

39
40
41 **Key Words:** FAM, loose mix aging, viscoelastic, fatigue, strain sweep, time sweep.

42 **HIGHLIGHTS**

- 43 • The LVE limit for STA and LTA aged FAM mixtures was found to be almost constant.
- 44 • Complex shear modulus ($|G^*|$) increased with a higher level of aging under lower and
45 intermediate reduced frequency.
- 46 • FAM mixtures aged at 95°C for 12 days and 135°C for 24 hrs showed similar response
47 for $|G^*|$ variation in lower and intermediate frequency zone.
- 48 • The fatigue properties of FAM mixtures decreased as the aging level changes from 5
49 days at 95°C to higher level aging of 12 days at 95°C.

1
2
3
4
5
6
7
8
9
10
11
12
13
14
15
16
17
18
19
20
21
22
23
24
25
26
27
28
29
30
31
32
33
34
35
36
37
38
39
40
41
42
43
44
45
46
47
48
49
50
51
52
53
54
55
56
57
58
59
60
61
62
63
64
65

1. Introduction

51 Fatigue cracking is considered as one of the major distress types to the flexible pavement.

52 Fatigue failure occurs due to repeated application of load and it becomes especially critical

53 for asphaltic pavements laid in intermediate to low temperature regions. Along with climatic

54 temperature, the aging characteristics of asphaltic mixture also play an important role in

55 controlling such cracks. An asphaltic mixture with a higher degree of susceptibility to aging

56 is expected to have lower design life and vice versa. Though aging phenomena is directly

57 related to the asphalt binder, various volumetric properties of asphaltic mixture play a critical

58 role in the overall aging process. For example, an asphaltic mixture with a higher amount of

59 air void is expected to have a higher degree of susceptibility to aging. Therefore, along with

60 study purely at asphalt binder level, it is equally important to understand the impact of aging

61 at asphaltic mixture level. Many research works have been reported which discusses the

62 effect of aging on various rheological performance parameters of asphalt binder [1–4].

63 Further, number of studies have been reported recently for the corresponding phenomena at

64 asphaltic mixture level too [5–10]. It is a usual practice to carry out aging in the laboratory

65 using different temperatures and aging periods to simulate the field aging of asphaltic

66 mixture. To simulate the Short Term Aging (STA), it is recommended to condition the

67 asphaltic mixture at 135°C for 4 hrs before compaction. Similarly, conditioning at 85°C for 5

68 days on compacted specimens has been recommended for simulating Long Term Aging

69 (LTA) of the asphaltic mixture (AASHTO R30). Additionally, NCHRP 09-54 recommended

70 laboratory aging of the loose mixture at 95°C and 135°C for different aging durations has

71 been reported by various researchers to study the aging effect on viscoelastic and fatigue

72 properties of asphalt concrete mixtures [11–18].

73 It is important to note that evaluating different viscoelastic properties, especially fatigue

74 performance of asphaltic mixture in the laboratory demands larger amount of materials,

1 75 expensive equipment and an appreciable amount of time for specimen preparation, aging
2 76 simulation, and performance testing. This has led the researchers in this area to look into
3
4 77 developing other methods which can address the limitations in evaluating the corresponding
5
6 78 viscoelastic properties at asphaltic mixture level to reduce the amount of material and
7
8 79 required time. The first attempt in this direction was made by Kim et al. [19] through
9
10
11 80 examining viscoelastic properties of Fine Aggregate Matrix (FAM) and this approach
12
13 81 reported to be cheaper, relatively simple, repeatable and less time consuming. It is important
14
15 82 to note that the FAM phase of the overall asphaltic mixture is critical as the crack formation
16
17 83 and propagation is largely governed by the viscoelastic properties of different materials
18
19 84 within this phase [20–22]. FAM is defined as the combination of fine aggregates, mineral
20
21 85 filler, and asphalt and have relatively more uniform structure compared to full asphalt
22
23 86 concrete mixture [23,24].
24
25
26
27
28

29
30 87 Till date, many studies have been conducted to investigate the role of FAM in characterizing
31
32 88 linear viscoelastic properties, time dependent behavior and fatigue properties in an overall
33
34 89 asphaltic mixture [25–28]. Karki et al. [25] used the micromechanical modeling approach to
35
36 90 predict the dynamic modulus of asphalt concrete mixtures and concluded that the FAM phase
37
38 91 can anticipate the viscoelastic properties of asphalt concrete mixtures. Underwood et al. [29]
39
40 92 studied the dynamic modulus and phase angle of FAM and full asphaltic mixture and
41
42 93 concluded that, the FAM mixtures found to have the sensitivity which is more in line with
43
44 94 that observed for full asphaltic mixtures under all of the tested conditions. The fatigue
45
46 95 cracking property of asphaltic concrete mixtures and FAM mixtures was further compared,
47
48 96 and similar ranking for fatigue life was observed for both the cases [30,31]. Overall, it may
49
50 97 be concluded that FAM mixture can be effectively used for characterizing the full asphaltic
51
52 98 mixtures in a qualitative way [20].
53
54
55
56
57
58
59
60
61
62
63
64
65

99 As mentioned earlier, aging changes the physical property of asphalt mixtures by increasing
100 stiffness, brittleness, and decreasing relaxation capability. Therefore, it is important to give
101 due consideration to aging phenomena at the mixture design stage to provide a durable
102 pavement structure. To achieve this problem, aging of asphaltic mixtures needs to be
103 simulated in the laboratory. Based on the extensive review of literature, to the best of the
104 knowledge to the authors, only a single research work till date has been reported which aimed
105 at understanding the effect of LTA on FAM mixture [32]. Laboratory compacted FAM was
106 conditioned at 85°C for 5 days to simulate long term aging as per AASHTO R30 before
107 evaluating fatigue property in their study. It is important to note that the aging process can be
108 accelerated with the help of increased conditioning temperature to reduce the conditioning
109 time in order to achieve the same degree of aging [10,33,34]. Since the standard protocol
110 recommends conditioning the specimen for 5 days which is a significantly longer time period,
111 however, it can be reduced by increasing the conditioning temperature. Such changes may
112 significantly save the conditioning time. Though the increase in conditioning temperature can
113 decrease the conditioning time, it is important to quantify the decrease in conditioning time
114 with a corresponding increase in conditioning temperature considering its influence on long
115 term performance parameter. This motivated the authors to investigate the impact of different
116 aging and conditioning time for different FAM to simulate the aging (long term aging) of
117 asphaltic mixture and the corresponding effect on different viscoelastic properties and long
118 term performance.

119 Therefore, the main objective of this study is to evaluate the various viscoelastic properties of
120 FAM mixtures aged using varied level of conditioning (by changing the temperature and
121 duration), including AASHTO R30 and newly recommended NCHRP 09-54 protocols for the
122 same. It is important to note that the amplitude strain level needs to be beyond the linear
123 viscoelastic range for inducing fatigue damage to the material. Therefore, strain sweep test

124 was initially conducted on various specimens conditioned at different aging levels to
125 demarcate the boundary line between linear and non-linear viscoelastic zone. Subsequently,
126 temperature and frequency sweep test was carried out on different specimens by applying
127 amplitude strain level within linear viscoelastic range which helped to examine the effect of
128 different aging level over a wide range of frequency by drawing the master curve for complex
129 shear modulus ($|G^*|$) and phase angle (δ) based on the Time-Temperature Superposition
130 (TTSP) principle. Finally, the fatigue property of FAM mixtures conditioned at different
131 aging level was evaluated using a time sweep test to reach an appropriate conclusive remark.

132 **2. Materials and FAM specimen preparation**

133 **2.1 Materials**

134 The FAM mixture is a combination of asphalt binder, fine aggregates and filler having size
135 less than 0.075 mm [21]. Following section briefly provides the information on basic
136 properties of different materials, specimen preparation and experimental methodology.

137 **2.1.1 Asphalt binder**

138 **Table 1.** Basic properties of asphalt binder

Property	Test Results	Limiting value IS 73:2013
Penetration at 25°C, 0.1 mm	64.5	Min. 45
Softening point (R&B) (°C)	52.7	45-55
Ductility at 25°C (cm)	85.4	Min. 70
Absolute viscosity at 60°C (poise)	2700	2400-3600
Kinematic viscosity at 135°C (cSt)	438	Min. 350
Flash Point (°C)	≥220	Min. 220

139 Viscosity grade asphalt binder (VG-30) provided by M/s Mangalore Refinery and
140 Petrochemicals Ltd. (Mangalore, India) was used as base binder. Basic properties of base
141 binder are listed out in Table 1. It is clear that the base binder satisfied the various
142 requirements set by IS: 73-2013. Moreover, the kinematic viscosity value of base binder at
143 135°C also satisfied the workability criteria set by Superpave (should be less than 3000 cSt).

144 **2.1.2 Aggregates**

145 To prepare FAM specimens throughout this study, single source granite aggregates obtained
146 from Kinnigoli Quarry, Dakshin Kannada District, Mangalore, India was used. The fine
147 aggregates smaller than 2.36 mm sieve size found to have specific gravity of 2.67. Similarly,

148 water absorption value was found to be 0.54%, satisfying the criteria ($\leq 2\%$) set by the
149 Ministry of Road Transportation and Highways (MoRTH 2013).

150 **2.1.3 Aggregate gradation for FAM mixtures**

151 The FAM aggregate gradation was designed based on the dense graded asphalt mixture with
152 a nominal maximum aggregate size of 19.0 mm. The FAM consists of the fine portion of the
153 full asphalt mixture with aggregates passing sieve 2.36 mm [29,32,35]. The usage of too
154 smaller aggregates passing 1.18 mm is not practical to prepare FAM specimens because,
155 large amount of fine materials are needed to prepare FAM specimens [32,35]. Also, FAM
156 specimens prepared using larger size aggregates passing 4.75 mm may cause variability in
157 test results [32,35]. Therefore, aggregates passing through 2.36 mm sieve were used for the
158 preparation of FAM specimens in this study. The HMA mix design and FAM gradation
159 [24,36–38] are shown in Fig. 1. The optimum binder content for the FAM mixtures was
160 determined with the help of surface area method [39–41]. Considering homogeneously coated
161 aggregates with asphalt binder having film thickness of 10 μ [19,24,42] the optimum binder
162 content for FAM mixture was found to be 7.3%. The target air void for various FAM
163 specimens was 4% ($\pm 1\%$) [24,25,43]. It is to be noted that the proportioning of fine aggregate
164 present in the FAM mixtures were kept the same as in the full HMA mixture aggregate
165 gradation. However, the amount of finer proportion of aggregate (smaller than 2.36 mm) was
166 normalized with respect to the largest size of aggregate used in the FAM (=2.36 mm) (Eq.1).

$$167 \quad \% \text{ passing sieve "x" in FAM} = \frac{\text{Mass of aggregate passing sieve "x" in full mixture}}{\text{Mass of aggregate passing sieve 2.36 in full mixture}} \times 100 \quad (1)$$

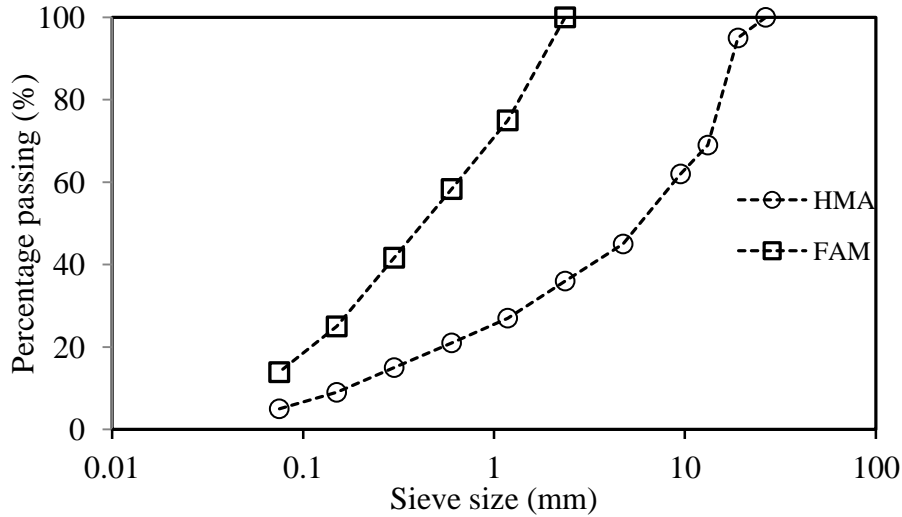


Fig. 1. Aggregate gradation for HMA and FAM mix design

2.1.4 FAM specimen preparation

Based upon the availability of resources and other laboratory constraints, either cylindrical or rectangular FAM specimens have been used by different researchers [35,44,45]. Rectangular shaped FAM specimens were prepared in this research work. Getting uniform, homogeneous and smooth surface of FAM specimen is important as it helps in obtaining repeatable results in the laboratory [20,44]. Such an approach for FAM specimen preparation not only produces specimens having smooth surfaces, but also save (a) significant lab space, (b) minimizes material wastage, and (c) saves significant time in mixing, compaction and cutting process. Initially, rectangular beam mould having a dimension of 50 mm x 12 mm x 10 mm as per ASTM D7552 guideline was fabricated. Subsequently, FAM specimens were prepared using a direct compaction method as recommended by Aragao et al. [46] and Nabizadeh et al. [47].

The mixing and compaction temperature were initially determined with the help of rotational viscometer as per ASTM D4402. Accordingly, the mixing and compaction temperature were found to be 153°C and 143°C respectively, satisfying the criteria for mixing temperature range (150-165°C) and compaction temperature should be minimum 140°C set by the

185 Ministry of Road Transportation and Highways (MoRTH 2013). The optimum asphalt binder
 186 content was initially mixed with the heated fine aggregate (see Fig. 2. for gradation) at the
 187 corresponding mixing temperature. Subsequently, STA of the loose mix was carried out for
 188 different FAM combinations at 135°C for 4 hrs as per AASHTO R30 recommendations.
 189 Further, theoretical maximum specific gravity (G_{mm}) of loose FAM mixtures was determined
 190 as per ASTM D2041. The G_{mm} of FAM specimen was found to be 2.21 g/cc at targeted air
 191 void. The FAM specimens were finally prepared by compacting (using static pressure) the
 192 required amount of loose mixture in the fabricated mould. A similar approach has been used
 193 by other researchers for the preparation of rectangular FAM specimens [44,46,47]. **The**
 194 **details of method to fabricate FAM specimens in this study adopted are shown in Table. 2.**

Table. 2. Details of method to fabricate FAM specimens

Steps	STA/LTA	Temperature	Time
Pre-heating of fine aggregates and asphalt binder		153°C	40 min
Mixing of loose FAM mixture			
Loose FAM mixture	STA	135°C	4 hrs
Loose FAM mixture	LTA	135°C	6, 12, and 24 hrs
Loose FAM mixture	LTA	95°C	5, and 12 days
Pre-heating of moulds		135°C	1 hr
Pre-heating		135°C	2 hrs
Compacting			
Compacted specimens	LTA	85°C	5 days
Cooling		AC room at 18°C	2 hrs
Extraction of specimens from the moulds			
Equilibration		Room temperature	24 hrs

196 Fig. 2 shows the various stages adopted during FAM specimen preparation. Specially
 197 provided fixture with Dynamic Shear Rheometer (DSR) was used to characterize each FAM
 198 specimens (Fig. 3). Utmost care was taken for FAM specimen while assembling in the DSR
 199 rectangular fixture so that it is well aligned and centred to avoid inconsistency of the obtained
 200 results.

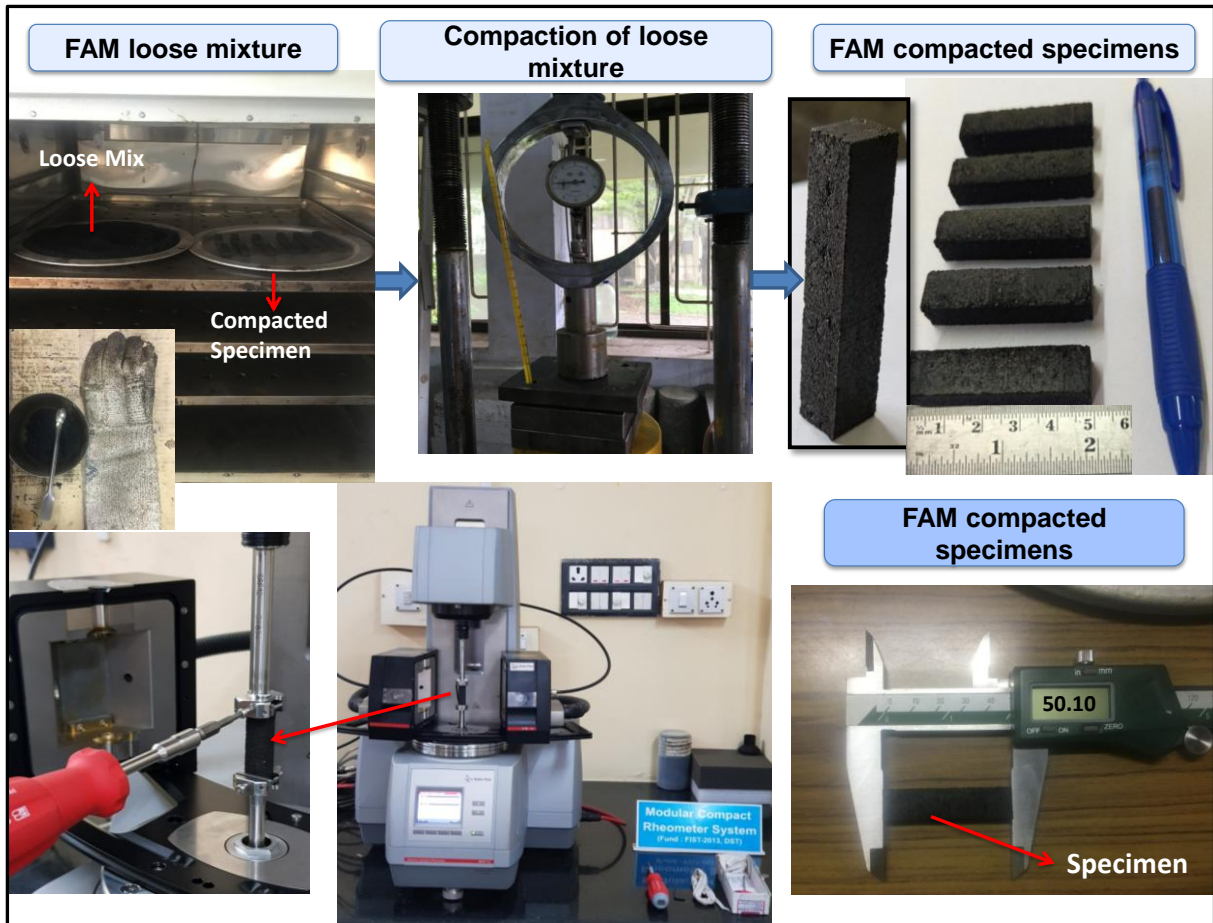


Fig. 2. Rectangular FAM Specimen Preparation

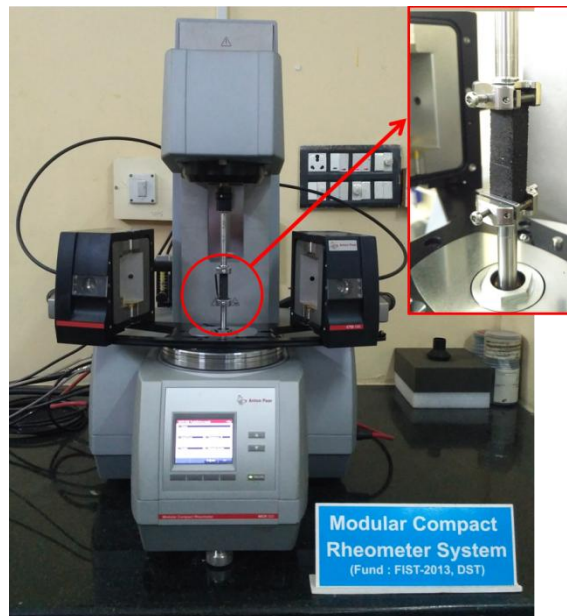


Fig. 3. Dynamic Shear Rheometer (MCR 502) Setup.

206 **2.2. Laboratory experimental plan**

207 This study aimed at evaluating the effect of different aging (loose mix aging and compacted
 208 specimen aging) levels on viscoelastic and fatigue properties of FAM mixtures. Short term
 209 aging on FAM loose mixture was carried out at 135°C for 4 hrs before compaction as per
 210 AASHTO R30 recommendation. To simulate long term aging, AASHTO R30’s current
 211 protocol recommends to carry out aging for 5 days at 85°C on compacted FAM specimens.
 212 Additionally, unlike AASHTO R30 recommendation, NCHRP 9-54 recommends long term
 213 aging on loose FAM for different aging duration and temperature (6 hrs at 135°C, 12 hrs at
 214 135°C, 24 hrs at 135°C, 5 days at 95°C and 12 days at 95°C). Therefore, along with
 215 AASHTO R30’s recommended protocol, long term aging of loose FAM was also carried out
 216 as per NCHRP 9-54 recommendation. Details of different FAM combinations, binder type,
 217 name of the test conducted, number of test specimens prepared and properties of FAM
 218 mixtures are shown in Table. 3. A, A1, A2, A3, B1, B2 refers to loose mixture aging,
 219 whereas, C’ refers to compacted specimen aging.

220 **Table. 3.** Details of Different FAM Combinations

Binder Type	Properties	Test Name	FAM Mixture Type							Number of Specimens
			Loose Mixture Aging						Compacted Specimen Aging	
			A	A1	A2	A3	B1	B2	C	
VG-30	Viscoelastic	Strain sweep	3	3	3	3	3	3	3	3x7=21
		Temp. and freq. sweep	3	3	3	3	3	3	3	3x7=21
	Fatigue	Time sweep @ 4 strain levels	3x4	3x4	3x4	3x4	3x4	3x4	3x4	3x4x7=84

221 Note: A=4 hrs at 135°C, A1=6 hrs at 135°C, A2=12 hrs at 135°C, A3=24 hrs at 135°C, B1=5 days at 95°C, B2=12 days at 95°C, C=5 days at 85°C, VG=Viscosity grade

222 Flowchart for the overall experimental plan is presented in Fig. 4. Three different types of
 223 strain controlled tests (strain sweep test, temperature, and frequency sweep test and time
 224 sweep test) were carried out on STA and LTA FAM specimens in this research work. Strain
 225 sweep test helped in demarcating the boundary line between linear and non-linear viscoelastic
 226 zone [20]. It is important to note that the temperature and frequency sweep test needs to be
 227 conducted by applying strain level in the linear viscoelastic range. Likewise, strain level in
 228 time sweep test for fatigue life analysis should be applied in non-linear viscoelastic range.
 229 Therefore, strain sweep test helped in selecting the appropriate strain level for temperature
 230 and frequency sweep and time sweep test.

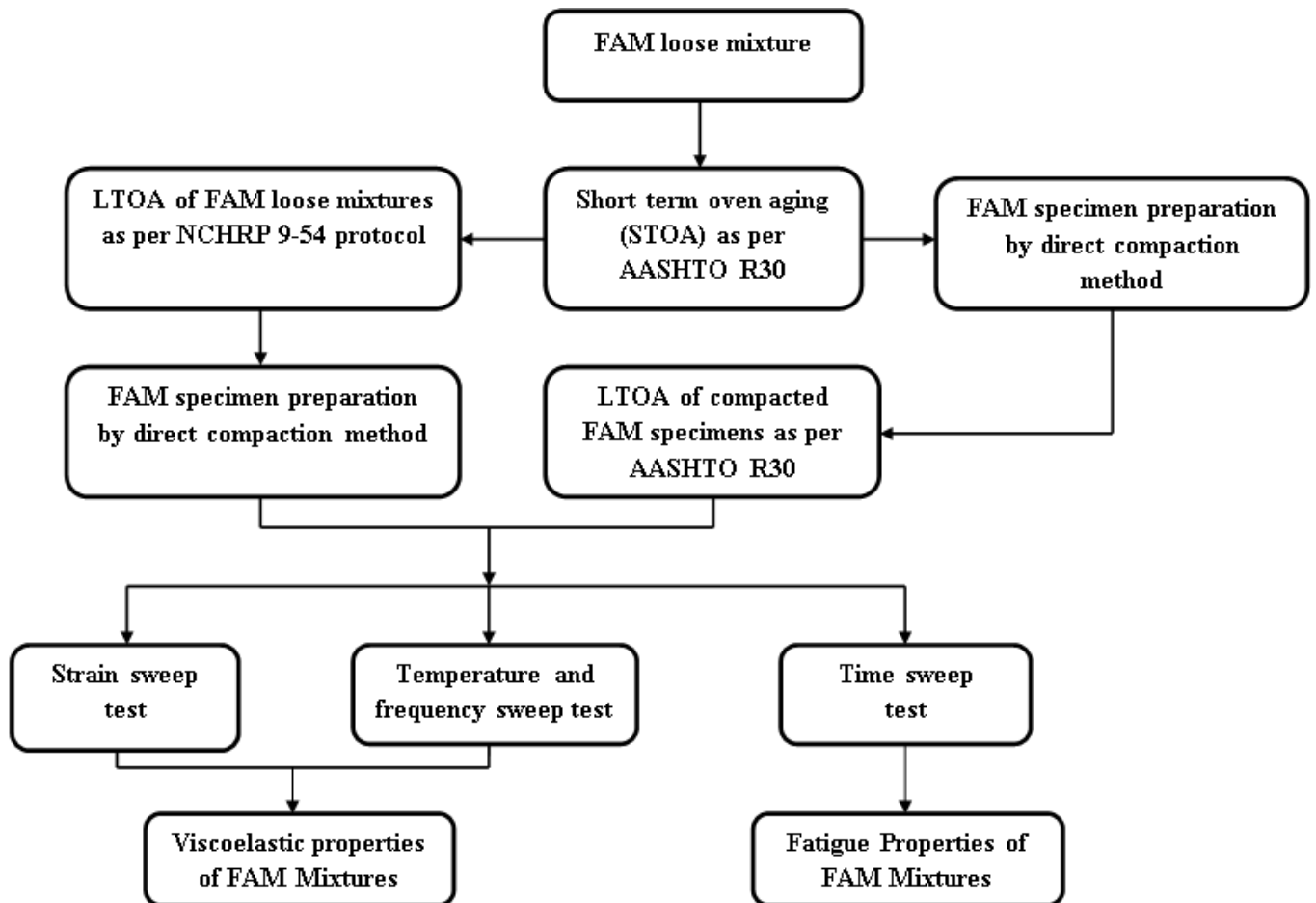


Fig. 4. Overall experimental plan

234 2.2.1 Linear viscoelastic region

1
2
3 235 Strain sweep test was carried out on both STA and LTA FAM specimens to determine the
4
5 236 linear viscoelastic region of each FAM mixture [46–48]. This test was conducted at a single
6
7
8 237 temperature and frequency level of 25°C and 10 Hz respectively by changing the strain levels
9
10 238 from 0.0001% - 0.1%. The idea behind choosing a single temperature (25°C) was due to the
11
12
13 239 fact that as the testing temperature increases, the strain corresponding to Linear Viscoelastic
14
15 240 (LVE) range increases. This approach ensured that this test was conducted at a selected strain
16
17
18 241 level at subsequently higher temperatures (higher than 25°C) are well within the LVE range.
19
20 242 Strain corresponding to a 10% drop in the $|G^*|$ was considered as maximum strain level under
21
22
23 243 LVE range.

26 2.2.2 Temperature and frequency sweep test

27
28
29 245 Temperature and frequency sweep test was conducted to determine the viscoelastic properties
30
31 246 of each FAM mixtures. Based on the LVE test results, constant strain level well within LVE
32
33
34 247 range was selected. The temperature was varied from 15°C to 65°C at the interval of 10°C,
35
36
37 248 whereas, frequency level was varied from 0.1 Hz to 25 Hz. The master curve for complex
38
39 249 shear modulus $|G^*|$ and phase angle δ was subsequently drawn. Williams-Landel-Ferry
40
41 250 (WLF) equation was used for finding out the reduced frequency at the reference temperature
42
43
44 251 25°C (Eq. 4) [29]. Logarithmic sigmoidal model was further used for drawing the master curve
45
46 252 for $|G^*|$ and δ at the reference temperature [15,16,29,49–51]. Eq. 2 shows the mathematical
47
48
49 253 form of the logarithmic sigmoidal model of $|G^*|$. In this study, the Lorentzian peak equation
50
51 254 was used to model the δ master curve accurately. Eq. 3 shows the Lorentzian peak model
52
53
54 255 equation for drawing the master curve for δ [17,52–54].

$$256 \log|G^*| = \alpha + \frac{\beta}{1 + e^{\gamma + \kappa(\log \omega_r)'}} \quad (2)$$

257 Where, α , β , γ , κ are the sigmoidal fitting coefficients which describe the shape of the $|G^*|$
 258 master curve and ω_r is the reduced frequency.

$$259 \text{ Phase angle } (\delta) = \frac{a \cdot b^2}{[(\log \omega_r - c)^2 + b^2]}, \quad (3)$$

260 The fit coefficients are a, b, and c as follows: ‘a’ indicates the peak value, ‘b’ controls the
 261 transition length, and ‘c’ is connected to the peak point horizontal position, δ is phase angle
 262 and ω_r is the reduced frequency.

$$263 \log a_T = \frac{C_1(T - T_R)}{C_2 + T - T_R}, \quad (4)$$

264 Where, T refers testing temperature ($^{\circ}\text{C}$), T_R is the reference temperature (25°C) and C_1 , C_2
 265 are the fitting coefficients.

266 2.2.3 Time sweep test

267 The strain controlled time sweep test was carried out on STA and LTA FAM specimens to
 268 characterise the fatigue cracking potential of FAM mixtures [21,32,38,39,46,47,55,56]. This
 269 test was conducted at four different strain levels (0.06%, 0.09%, 0.12% and 0.15%)
 270 (Considering temperature = 25°C , and frequency = 10 Hz) in non LVE range to cause
 271 sufficient fatigue damage to the FAM mixture [19,21,44,57]. Number of cycles at 50%
 272 reduction in the $|G^*|$ value was considered to be fatigue failure of FAM specimens [58–60].
 273 Considering three replicate specimens, time sweep test was conducted on a total of 84
 274 specimens to examining the fatigue potential of FAM mixture. Fatigue test results can be
 275 described by a phenomenological regression model as described by Eq. 8 [19].

$$276 N_f = a(\gamma)^b \quad (8)$$

277 Where, N_f = Fatigue life, γ = Applied non-LVE strain level, and a, b= Regression coefficients.

278 3. Test Results and Analysis

279 3.1 Linear viscoelastic region

280 This test has been reported by various researchers for different types of FAM mixtures which
281 helped in determining the LVE range for various specimens in this research work. The results
282 of the strain sweep test on various FAM specimens are presented in Fig. 5. The curves of $|G^*|$
283 versus strain from the strain sweep test has been plotted for FAM mixtures with different
284 aging levels. It is clear from the plot that as the aging level increased, the stiffness value also
285 increased. For example, the stiffness value within LVE range can be observed to be increased
286 by approximately two times with a change in aging protocol from A (short term aging at
287 135°C for 4 hrs) to B2 (12 days aging at 95°C) (refer Table 2 for specimen nomenclature).
288 Moreover, it is also to be noted that the $|G^*|$ plot for specimen aged for 12 days at 95°C
289 overlapped with the corresponding plot with specimen aged at 135°C for 24 hrs (A3) within
290 the LVE range. Such a response indicates the equivalency of aging level of FAM between (a)
291 12 days at 95°C and (b) 135°C for 24 hrs. This result is important in the sense that the aging
292 period can be significantly reduced from 12 days to just 24 hrs just by increasing the
293 conditioning temperature from 95°C to 135°C. It can be further seen that the $|G^*|$ value
294 remained constant when the applied strain level is within the LVE range. However, as soon
295 as strain level increased above the corresponding LVE range of specimen, the decrease in
296 $|G^*|$ became apparent as expected. Such a response clearly indicates the requirement of
297 amplitude strain level above the respective LVE limit to induce damage to the material.
298 Irrespective of the aging level applied to the specimen, it is to be noted that the LVE range
299 remained almost constant ($\approx 0.006\%$). The results are in line with the findings reported by
300 Aragão and Kim [27] and Li et al. [39] where LVE range was found to be insensitive to the
301 induced aging level to the FAM specimens.

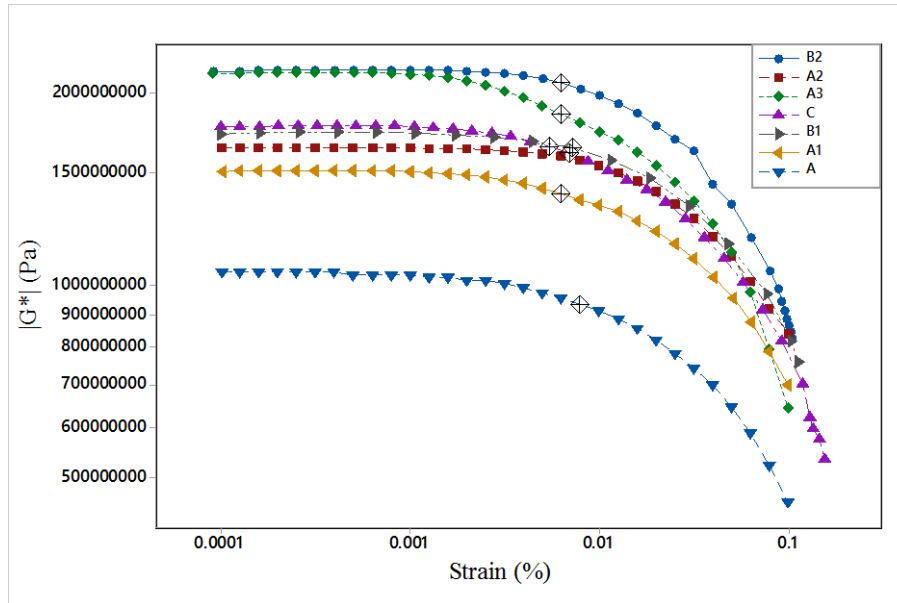


Fig. 5. Results of FAM strain sweep test

3.2 Temperature and frequency sweep test

Based on the outcome obtained from strain sweep test as discussed earlier, temperature and frequency sweep test was carried out by applying an amplitude strain level within the LVE range. The master curve for $|G^*|$ for seven different FAM mixtures with STA and LTA (A, A1, A2, A3, C, B1 and B2) was drawn at a reference temperature of 25°C with the help of time-temperature superposition principle and logarithmic sigmoidal model. Various model parameters which control the shape of the master curve were obtained from the solver function available with Microsoft Excel through optimization technique. The various model parameters obtained from the optimization technique for different FAM specimens are presented in Table. 4. Each plot represents the average of three replicates specimens. γ value in the generalized sigmoidal model governs the horizontal positioning of turning point [50]. It is clear from the table that as the aging level increased, the γ value correspondingly decreased. For example, the γ value for A1 specimens is -0.33 which decreased to -0.43 and -0.56 with an increase in aging duration from 6 hrs to 12 and 24 hrs respectively. Such a response can be attributed to the stiffening effect to the FAM specimen due to increase in the

319 relative proportion of asphaltene and a corresponding decrease in maltene in asphalt binder
 320 used in FAM with an increase in aging temperature and/or corresponding aging duration [50].
 321 Likewise, other parameters of the logarithmic sigmoidal model also seem to be affected by
 322 different aging protocol to the FAM specimen. For example, κ and β value can be seen to be
 323 increasing with an increase in aging level except to the case of β value when aging level at
 324 135°C increased from 12 to 24 hrs.

Table. 4. Complex shear modulus $|G^*|$ master curve parameters of FAM mixtures

Mixture Type	α	β	γ	κ
A	7.04	2.73	-0.15	-0.55
A1	6.78	3.47	-0.33	-0.31
A2	6.79	3.58	-0.43	-0.28
A3	7.32	2.65	-0.56	-0.30
C	6.97	3.19	-0.22	-0.40
B1	6.84	3.35	-0.35	-0.36
B2	6.33	4.23	-0.57	-0.22

327 Fig. 6 shows the master curve for different FAM mixtures. Increase in $|G^*|$ value with
 328 increase in frequency level can be observed as expected. Each plot can be seen as
 329 approaching towards a single value at higher frequency level which can be attributed to
 330 attainment of glassy state of the mixture and in line with findings on FAM mixtures reported
 331 by different researchers [17,43,55]. On the other hand, the apparent effect of aging can be
 332 clearly seen in relatively lower frequency zone. The lowest value of $|G^*|$ can be observed for
 333 STA specimen which subsequently increased with the increase in different aging level. For
 334 example, $|G^*|$ value of A3 mixture aged at 24 hrs at 135°C is about 8.8 times more than the
 335 STA FAM mixture at a frequency level of (0.00005 rad/s). Similarly, $|G^*|$ value of specimen
 336 aged for 5 days at 95°C (B1) loose mixture aged FAM specimen showed 2.5 times stiffer
 337 compared to STA FAM mixture at a frequency level of (0.00005 rad/s). Moreover, the
 338 specimen C (conditioned at 85°C for 5 days) found to have almost similar response as that of

339 specimen B1 (conditioned at 95°C for 5 days) except at very low frequency level where the
340 corresponding value for B1 can be seen as slightly higher than C. Similar findings has been
341 reported by Rahbar-Rastegar et al. [17] for asphaltic mixture with different degree of aging.
342 A higher value of $|G^*|$ for B1 in lower frequency range can be attributed to correspondingly
343 higher conditioning temperature leading to a relatively higher degree of aging. Further, as in
344 the case of amplitude sweep test (conducted at a frequency level of 10 Hz), where $|G^*|$
345 variation for specimen B2 (conditioned at 95°C for 12 days) and specimen A3 (conditioned at
346 135°C for 24 hrs) in LVE range was found to be similar. Response for the corresponding
347 specimens can be seen to be in close proximity at a reduced frequency level of 10 Hz which
348 is in agreement with findings obtained from strain sweep test as discussed in Section 3.1.
349 However, at a relatively lower frequency and higher frequency level, the response can be
350 seen as different. The $|G^*|$ value for A3 is relatively higher than B2, whereas, the
351 corresponding value at a higher frequency level for B2 is higher than A3. This indicates that
352 specimen A3 may perform better than B2 in high temperature condition (equivalent to low
353 frequency), whereas, the specimen A3 may perform better than B2 in low to intermediate
354 temperature conditions. Fig.7 shows the variation of $|G^*|$ value at 0.001 Hz to demonstrate
355 the effect of different aging level on corresponding parameter in lower frequency zone.

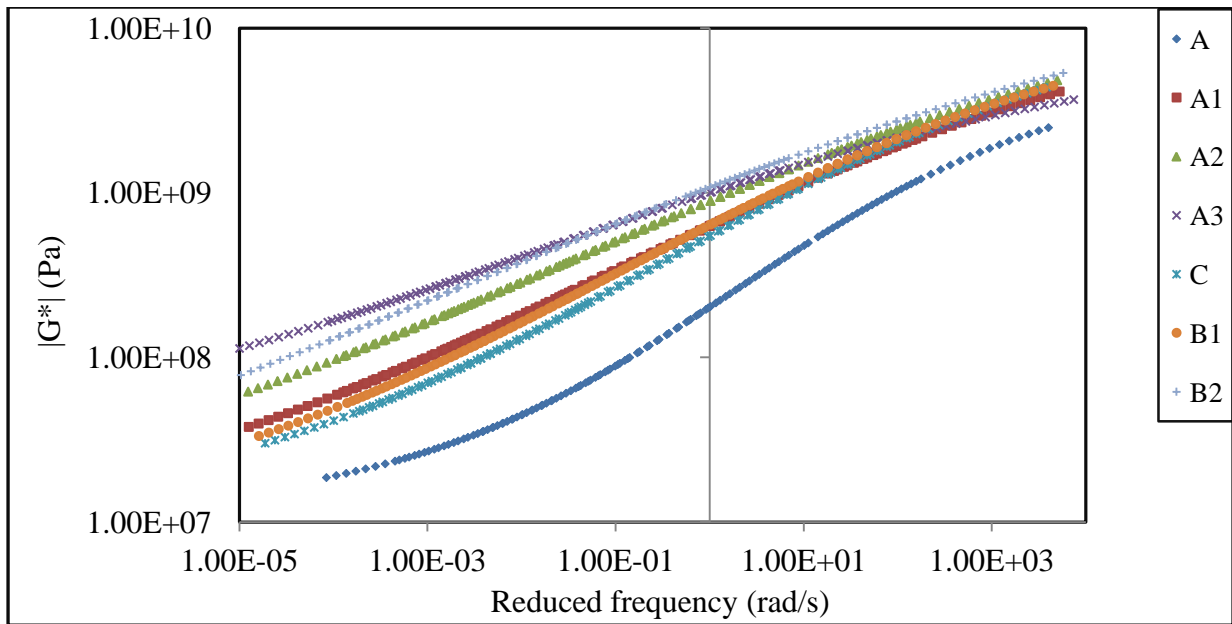


Fig. 6. Complex shear modulus $|G^*|$ of STOA and LTOA FAM mixtures at reference temperature 25°C.

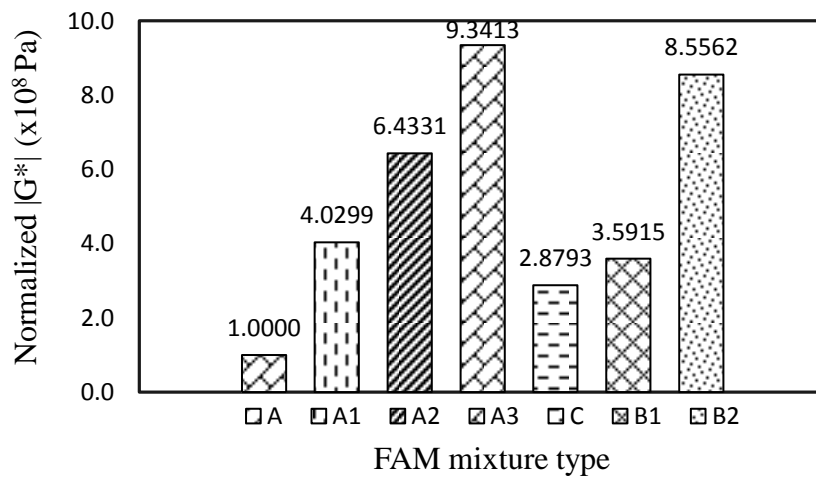


Fig. 7. Normalised $|G^*|$ of FAM mixtures at 0.001Hz and 25°C.

The $|G^*|$ master curve exhibit a characteristic flattening effect that can be quantified by the slope (m) of the logarithmic plot between $|G^*|$ and frequency (known as relaxation modulus) [61,62] was also are determined as shown in Table 5, m -values between each FAM mixtures at different frequency levels has been compared. The values in Table 4 clearly demonstrate the influence of aging on the m -values at higher temperature (or lower frequencies). The

366 long-term aged FAM mixtures found to have distinctively different relaxation time compared
 367 with the STA FAM mixtures. Generally, the aged FAM mixtures take more stress relaxation
 368 time than the STA mixtures [47]. The increase in m-values may be attributed to increase in
 369 aging level to FAM specimen. For example, A3 mixture aged at 24 hrs at 135°C is having
 370 higher m-value compared to STA FAM mixture at a lower side of reduced frequency level.

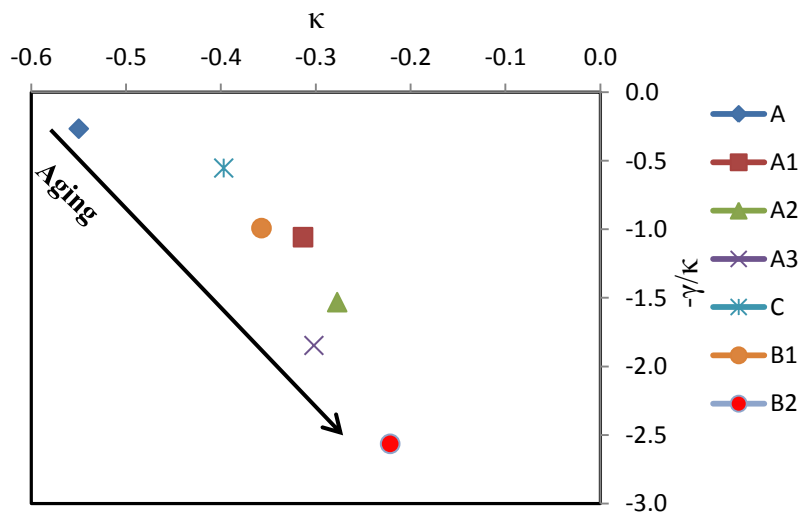
371 **Table. 5.** Slope between each FAM mixtures at different frequency levels

Mixture Type	Slope, m		
	At lower reduced frequency (0.00005 rad/s)	At intermediate reduced frequency (1.5 rad/s)	At higher reduced frequency (5250 rad/s)
A	0.018	0.069	0.170
A1	0.394	0.158	0.190
A2	0.678	0.197	0.222
A3	1.202	0.167	0.078
C	0.187	0.158	0.297
B1	0.275	0.177	0.240
B2	1.323	0.217	0.205

372 Similarly, 5 days at 95°C (B1) loose mixture aged FAM specimen showed higher m-value
 373 compared to STA FAM mixture at a lower side of reduced frequency level. Further, m-values
 374 increase at intermediate side of reduced frequency levels. Moreover, the effect of aging levels
 375 at low temperature or high loading frequencies was not distinguishable. This indicates that
 376 highly aged FAM mixtures can be more susceptible to early stage fatigue damage due to lack
 377 of relaxation capability. The results are in line with findings reported by Sanchez et al. [49]
 378 for different FAM.

379 Furthermore, inflection point parameter ($-\gamma/\kappa$) and relaxation width parameter (κ) from the
 380 $|G^*|$ master curve plot are considered to analyse the relationship between aging duration and
 381 temperature. However, the ' κ ' value influences the length of the relaxation spectra and it is
 382 possible to calculate the frequency of the inflection point from $10^{-\gamma/\kappa}$. As the asphalt material
 383 ages, the $|G^*|$ master curve tends to flatten and the inflection point shifts to lower frequencies
 384 [63]. The $(-\gamma/\kappa)$ parameter for STA FAM mixture (A) is almost equal to zero. Similarly, $-\gamma/\kappa$

385 value of specimen aged for 5 days at 95°C (B1) loose mixture aged FAM specimen showed
 386 3.97 times more compared to STA FAM mixture. Moreover, the specimen C (conditioned at
 387 85°C for 5 days) found to have almost similar response as that of specimen B1 (conditioned
 388 at 95°C for 5 days). The corresponding value for B1 (-0.991) can be seen as slightly higher
 389 than C (-0.553). Similar findings have been reported by Rahbar-Rastegar et al.[17] for
 390 asphaltic mixture with different degree of aging. A higher value of $-\gamma/\kappa$ for B1 in can be
 391 attributed to correspondingly higher conditioning temperature leading to a relatively higher
 392 degree of aging. It is clear from the Fig. 8 that as the aging level increased, the $-\gamma/\kappa$ value
 393 correspondingly increased. For example, the $-\gamma/\kappa$ value for A1 specimens is -1.058 which
 394 increased to -1.531 and -1.847 with an increase in aging duration from 6 hrs to 12 and 24 hrs
 395 respectively. The $-\gamma/\kappa$ parameter decreases and κ increases, as more aging happens, pushing
 396 points further towards the bottom right. Such a response can be attributed to the stiffening
 397 effect to the FAM specimen with an increase in aging temperature and/or corresponding
 398 aging duration. These can also indicating that FAM mixtures with higher κ values are
 399 expected to be more susceptible to cracking [7,63].



401 **Fig. 8.** Variations of $|G^*|$ master curve shape parameter with different aging levels at a
 402 reference temperature of 25°C.

1
2
3
4
5
6
7
8
9
10
11
12
13
14
15
16
17
18
19
20
21
22
23
24
25
26
27
28
29
30
31
32
33
34
35
36
37
38
39
40
41
42
43
44
45
46
47
48
49
50
51
52
53
54
55
56
57
58
59
60
61
62
63
64
65

403 The master curve of δ for each STA and LTA specimen was also drawn as shown in Fig. 9.
404 Unlike the variation of $|G^*|$, a distinct change in δ with a change in reduced frequency can be
405 seen. It is clear from the plot that as the aging level increased to the FAM mixture, the
406 corresponding value at a particular frequency level decreased, indicating decreases in
407 relaxation property of the FAM specimen. Such a response can be attributed to the
408 viscoelastic nature of the FAM mixture which further indicates the increase in susceptibility
409 of FAM towards cracking with an increase in aging level. For example, the maximum value
410 of δ of specimen A is approximately twice the corresponding maximum value of specimen
411 A3. Likewise, a similar decrease in δ value can be obtained with different aging level. In the
412 majority of the cases, δ value can be seen as increasing with the increase in reduced
413 frequency which subsequently decreased with a further decrease in reduced frequency level.
414 It indicates the importance of loading frequency in the behavior of the FAM mixture. Such a
415 response for the variation of δ over the wide range of frequency is in agreement with findings
416 on FAM reported by Rastegar et al. [17] and Underwood and Kim [29]. It is also interesting
417 to note that as the aging level increased to the FAM specimen, the flatness of the
418 corresponding plot for δ value increased. In other words, the increase in an aging level
419 decreased the degree of dependency of δ value on loading frequency. For example, among A,
420 A1, A2, and A3 specimen, the flatness of δ plot over reduced frequency is highest for A3.
421 Similar response for δ can be seen between specimen C and B1. Such a response may be
422 attributed to the increased effect of elastic aggregate structure in overall material response;
423 however, it could also be related to the limitations of linear viscoelastic principle in
424 describing the behavior of FAM mixture, especially for highly aged specimens. Similar to the
425 case of $|G^*|$, the statistical analysis for the variation of δ was also carried out and variation
426 was found to be within an acceptable range and shown in Table. 7.

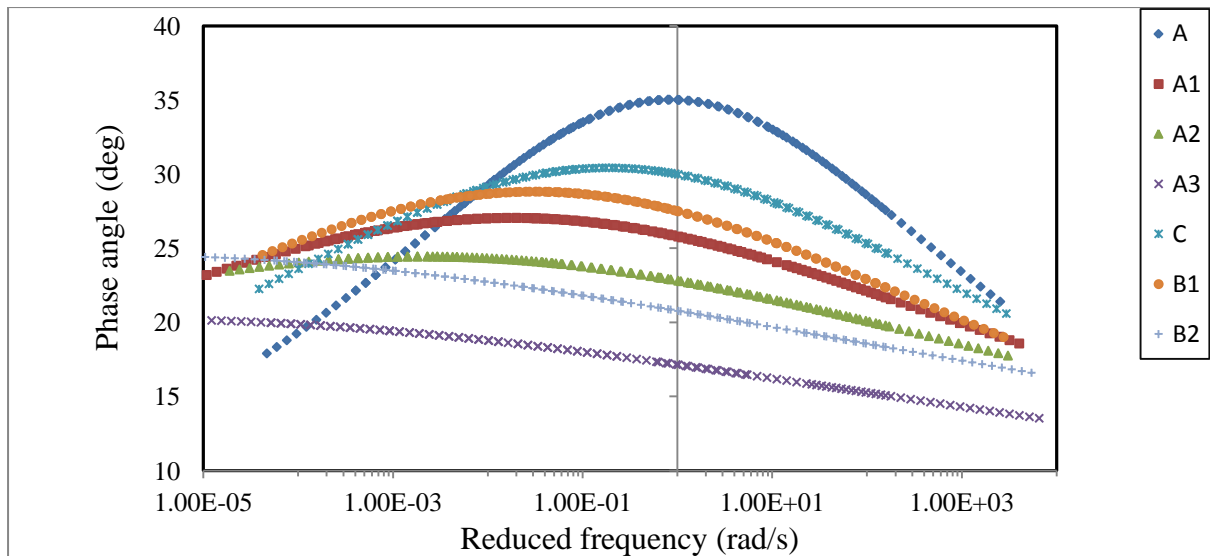


Fig. 9. Phase angle of STA and LTA FAM mixtures at a reference temperature of 25°C.

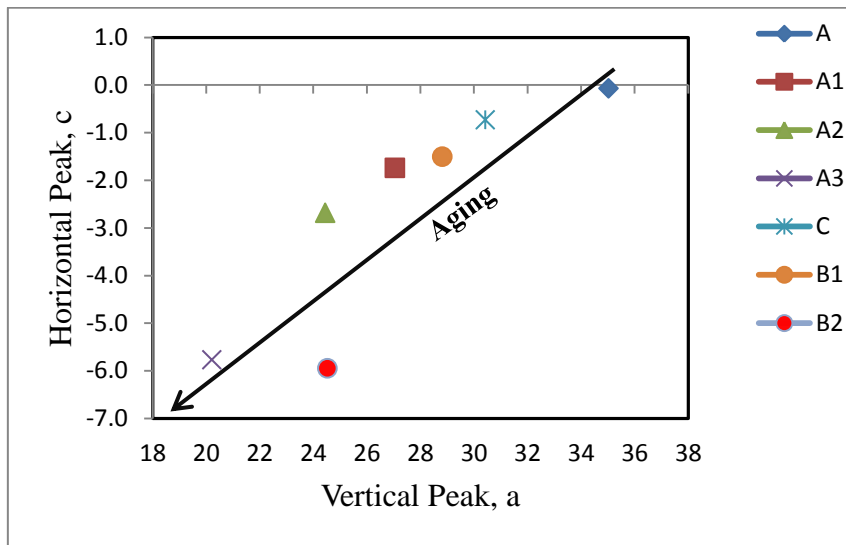
Further, for more analysis of relation between aging duration and temperature used in this study, the variation of the vertical position of peak (a) and the parameter related to the horizontal position of peak (c) with aging were selected. Fig. 9 can be an indicator for the relaxation potential of the FAM mixtures aged at different duration and temperature levels. Further, Fig. 10 clearly showed that how both vertical and horizontal peak values decline as the aging level increases, shifting the points to the plot's lower left. FAM mixtures with higher horizontal and vertical peak values are expected to have higher relaxation capability and better fatigue behaviour. 'A' has higher vertical peak values (a) and horizontal peak (c). This indicates that, 'A' have higher relaxation capability and better fatigue behaviour compared to A3. The various model parameters obtained from the optimization technique for different FAM specimens are presented in Table. 6. Each plot represents the average of three replicates specimens.

444

Table. 6. Phase angle master curve parameters of FAM mixtures

Mixture Type	a	b	c
A	35.02	-4.36	-0.07
A1	27.04	-7.91	-1.74
A2	24.44	-10.05	-2.68
A3	20.21	-13.64	-5.77
C	30.42	-6.08	-0.73
B1	28.81	-6.88	-1.50
B2	24.52	-14.01	-5.95

445



446

Fig. 10. Variations of δ master curve shape parameter with different aging levels at a reference temperature of 25°C.

447

448

449 Finally, the various values obtained from the modeling were statistically compared with the
 450 corresponding experimental values and the goodness of fit was evaluated for each FAM
 451 specimen. The statistical analysis results are provided in Table. 7. It can be clearly seen that
 452 the goodness of fit parameters obtained for different specimens are well within the acceptable
 453 range.

454

455

456

Table. 7. Goodness-of-fit results of $|G^*|$ and δ from master curve analysis

Mixture Type	$ G^* , R^2$	Acceptance criteria, [50,64]	δ, R^2	Acceptance criteria, [50,64]
	Coefficient of determination	Coefficient of determination	Coefficient of determination	Coefficient of determination
A	0.997	Excellent (≥ 0.90)	0.87	Good (0.70-0.89)
A1	0.990	Excellent (≥ 0.90)	0.71	Good (0.70-0.89)
A2	0.827	Good (0.70-0.89)	0.71	Good (0.70-0.89)
A3	0.900	Excellent (≥ 0.90)	0.93	Excellent (≥ 0.90)
C	0.975	Excellent (≥ 0.90)	0.73	Good (0.70-0.89)
B1	0.974	Excellent (≥ 0.90)	0.70	Good (0.70-0.89)
B2	0.990	Excellent (≥ 0.90)	0.84	Good (0.70-0.89)

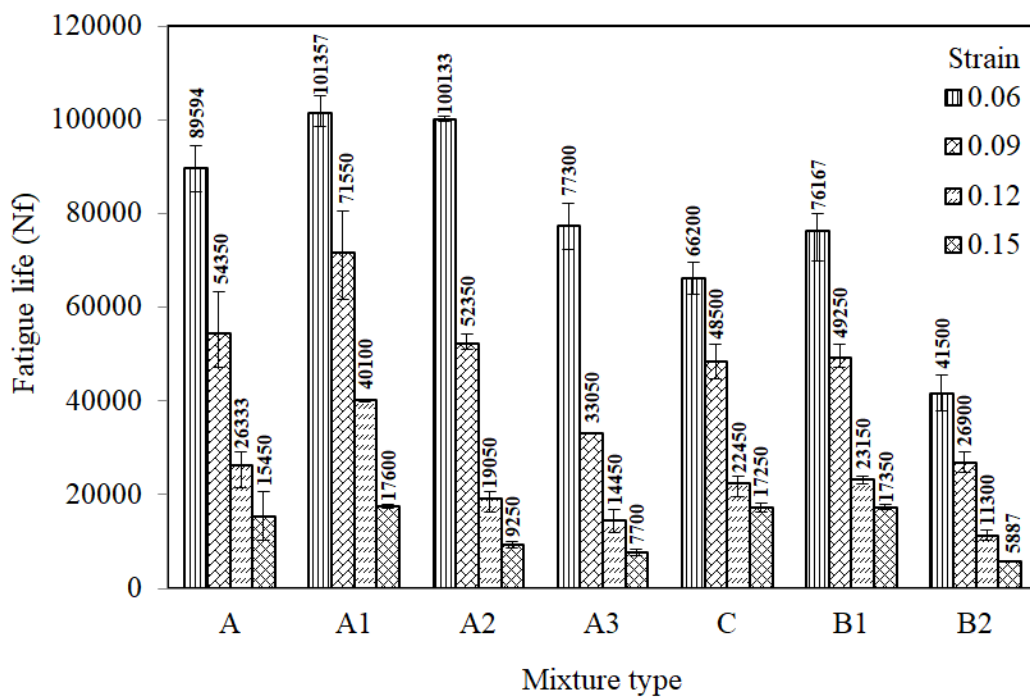
457

3.3 Time sweep test results

To examine the effect of different aging protocols on fatigue life, time sweep test under strain controlled (0.06%, 0.09%, 0.12% and 0.15%) condition was carried out at 25°C using constant frequency level of 10Hz [19,20]. Reduction in $|G^*|$ value by 50% of its initial value is widely accepted criteria for defining the end of the fatigue life of the specimen and the same has also been adopted in this research work [42,59,60].

The fatigue life of each FAM mixtures at different strain levels is shown in Fig. 11. The average fatigue life and corresponding Coefficient of Variation (COV) for various FAM combinations are also provided in the plot. The maximum COV was found to be 27.7% for specimen 'A' which is well below an acceptable value of 30% [45]. It is clear that the fatigue life of FAM mixtures are varying with different strain levels and aging levels. Irrespective of the aging level of a particular FAM specimen, an increase in strain level decreased the fatigue life as expected. For example, an increase in strain level from 0.06% to 0.15% for A3 specimen decreased the average fatigue life from 77300 to 7700, indicating a decrease in

472 fatigue life by 90.03%. Similar results can be obtained for other FAM specimens at other
 473 strain levels. Further, as the aging level to FAM mixture increased, except the case of
 474 increase in aging level from A to A1 (for which unexpectedly increased fatigue life is
 475 evident) similar findings were observed in these studies [65,66], decrease in fatigue life can
 476 be clearly seen. For example, an increase in aging level from A to A3 decreased the fatigue
 477 life from 54350 to 33050 at 0.09% strain level, indicating the decrease in corresponding value
 478 by 39.19%. Further, the comparison of different aging protocols based on fatigue life of FAM
 479 mixtures is shown in Fig. 11. The trend of different aging level protocols showed that the
 480 fatigue life of FAM specimen aged at 5 days for 95°C have more fatigue life than FAM
 481 specimen aged for 12 days at 95°C, and 24 hrs at 135°C. The FAM specimen aged for 24 hrs
 482 at 135°C showed better fatigue life than specimen aged for 12 days aged at 95°C. The
 483 potential reason for such response might be due to the presence of relatively higher amount of
 484 already aged and oxidized asphalt binder present in these FAM mixtures.



485
486 **Fig. 11.** Strain controlled fatigue test results at 25°C and the frequency of 10Hz

487 Further, the fatigue life of each STA and LTA FAM mixtures was predicted by using
 488 regression analysis. The model coefficients obtained from regression analysis is presented in
 489 Table. 8.

490 The fatigue model regression coefficients ‘a’ and ‘b’ are derived on the basis of measurable
 491 material parameters [21]. It is clear that the fatigue life of FAM mixtures are varying with
 492 different strain and aging levels. It is to be noted that the fatigue model coefficients (a and b)
 493 value decreased with increase in aging level in general except to the case of increase in aging
 494 level from A to A1 which may be attributed to unexpectedly higher fatigue life for A1
 495 compared to A. For example, the ‘a’ value for A1 specimens is 679.020 which decreased to
 496 71.845 and 27.406 with an increase in aging duration from 6 hrs to 12 and 24 hrs
 497 respectively. Further, an improper trend of regression coefficients can be seen with respect to
 498 different aging protocols at 95°C and 135°C. This indicates the combined effect of regression
 499 coefficients ‘a’ and ‘b’ on overall fatigue life of FAM mixtures.

Table. 8. Fatigue model regression coefficients

Mixture type	Fatigue model regression coefficients	
	a	b
A	430.790	-1.934
A1	679.020	-1.840
A2	71.845	-2.627
A3	27.406	-2.861
C	924.390	-1.553
B1	708.080	-1.689
B2	283.650	-1.815

502 **Summary of Findings.**

1
2
3 503 The aging of FAM mixtures was performed based on the AASHTO R30 and NCHRP 09-54
4
5 504 recommendations. Effect of aging on $|G^*|$ and δ at larger temperature range and frequencies
6
7
8 505 were evaluated by conducting temperature and frequency sweep test. Results were compared
9
10 506 through constructing master curves for each FAM mixtures at reference temperature 25°C.
11
12
13 507 Further, fatigue performance of FAM mixtures at intermediate temperature 25°C and four
14
15 508 different strain levels were evaluated using time sweep test. Results of fatigue cracking
16
17
18 509 potential of each FAM mixtures at different aging levels and strains by considering 50%
19
20 510 reduction in the initial stiffness $|G^*|$ values were compared. The findings of this study are
21
22
23 511 summarized below:

- 24
25
26 512 • The LVE limit for STA and LTA aged FAM mixtures was found to be almost constant.
27
28 513 This indicates that the LVE range was found to be insensitive to the induced aging level
29
30
31 514 to the FAM specimens.
- 32
33 515 • The $|G^*|$ value of B2 (aged for 12 days at 95°C) specimen within the LVE range was
34
35
36 516 observed to be double of the corresponding value for STA (aged for 4 hrs at 135°C)
37
38 517 specimen. Also, $|G^*|$ plot for specimen B2 overlapped with the corresponding plot with
39
40
41 518 specimen A3 within LVE range. This indicates the equivalency of aging level of FAM
42
43 519 mixtures A3 and B2.
- 44
45 520 • The $|G^*|$ master curve plot showed that the A3 specimen had $|G^*|$ value 8.8 times more
46
47
48 521 compared to STA specimen at a lower frequency zone. Such a response was attributed to
49
50 522 the stiffening effect to FAM specimens due to increase in the relative proportion of
51
52
53 523 asphaltene and a corresponding decrease in maltene in asphalt binder used in FAM with
54
55 524 an increase in aging temperature and aging duration.

- 1
2
3
4
5
6
7
8
9
10
11
12
13
14
15
16
17
18
19
20
21
22
23
24
25
26
27
28
29
30
31
32
33
34
35
36
37
38
39
40
41
42
43
44
45
46
47
48
49
50
51
52
53
54
55
56
57
58
59
60
61
62
63
64
65
- 525 • The $|G^*|$ value of A3 from master curve was found to be higher than B2 at lower
526 frequency zone. Whereas, $|G^*|$ value of B2 was observed more than A3 at higher
527 frequency level. This indicates that specimen A3 may perform better than B2 specimen
528 in higher temperature condition and specimen B2 may perform better in low to
529 intermediate temperature conditions.
 - 530 • FAM mixtures aged at 95°C for 12 days and 135°C for 24 hrs showed similar response
531 for $|G^*|$ variation in lower and intermediate frequency zone, indicating the equivalencies
532 of their respective aging protocol.
 - 533 • Increase in aging level decreased the degree of dependency of δ value on loading
534 frequency. Among A, A1, A2, and A3 specimen, the flatness of δ plot over reduced
535 frequency was observed to be highest for A3. Such a response may be attributed to the
536 increased effect of elastic aggregate structure in overall material response.
 - 537 • The master curve parameters, $-\gamma/\kappa$ decreased and κ increased, as more aging happens,
538 such a response can be attributed to the stiffening effect to the FAM specimen with an
539 increase in aging temperature and/or corresponding aging duration. These can also
540 indicate that FAM mixtures with higher κ values are expected to be more susceptible to
541 cracking.
 - 542 • The fatigue life of 24 hrs at 135°C aged FAM mixtures showed better fatigue life than 12
543 days aged at 95°C FAM mixtures. The potential reason for such response might be due
544 to the presence of relatively higher amount of already aged and oxidized asphalt binder
545 present in these FAM mixtures.
 - 546 • The fatigue properties of FAM mixtures decreased as the aging level changes from 5
547 days at 95°C to higher level aging of 12 days at 95°C. Despite of the similar viscoelastic
548 properties, the trend observed between FAM mixtures aged 12 days at 95°C and 24 hrs at
549 135°C were not found to have similar fatigue properties.

550 These findings are based on the effect of different aging levels on FAM mixture prepared
1
2 551 with only one binder type. However, the plan of this study is to expand the work to evaluate
3
4 552 the effect of different aging levels on viscoelastic and fatigue properties of FAM mixtures
5
6 553 prepared with different binder type, aggregates and mineral fillers. Further, permanent
7
8 554 deformation and moisture damage study can also be carried out on different FAM mixtures.
9
10
11
12
13
14
15
16
17
18
19
20
21
22
23
24
25
26
27
28
29
30
31
32
33
34
35
36
37
38
39
40
41
42
43
44
45
46
47
48
49
50
51
52
53
54
55
56
57
58
59
60
61
62
63
64
65

555 **Acknowledgement**

1
2
3 556 Authors would like to acknowledge the financial support extended by the Department of
4
5 557 Science and Technology, Government of India under the scheme ‘Fund for Improvement of
6
7
8 558 Science & Technology infrastructure’ (No.SR/FST/ETI-356/2013) for the creation of
9
10 559 required research facilities at the Advanced Asphalt Characterisation and Rheology
11
12
13 560 Laboratory, Department of Civil Engineering, National Institute of Technology Karnataka,
14
15 561 India.
16
17
18
19
20
21
22
23
24
25
26
27
28
29
30
31
32
33
34
35
36
37
38
39
40
41
42
43
44
45
46
47
48
49
50
51
52
53
54
55
56
57
58
59
60
61
62
63
64
65

562 **REFERENCES**

- 1
2
3 563 [1] M.W. Mirza, M.W. Witczak, Development of a Global Aging System for Short and
4
5 564 Long Term Aging of Asphalt Cements, *Journal of the Association of Asphalt Paving*
6
7 565 *Technologists*. 64: (1995), 393–430.
8
9
10 566 [2] Y. Ruan, R.R. Davison, C.J. Glover, The effect of long-term oxidation on the
11
12 567 rheological properties of polymer modified asphalts, *Fuel*. (2003). doi:10.1016/S0016-
13 568 2361(03)00144-3.
14
15
16 569 [3] M. Ling, X. Luo, F. Gu, R.L. Lytton, Time-temperature-aging-depth shift functions for
17
18 570 dynamic modulus master curves of asphalt mixtures, *Constr. Build. Mater.* (2017).
19
20 571 doi:10.1016/j.conbuildmat.2017.09.156.
21
22 572 [4] P.K. Ashish, D. Singh, S. Bohm, Investigation on influence of nanoclay addition on
23
24 573 rheological performance of asphalt binder, *Road Mater. Pavement Des.* 0629 (2016) 1–
25
26 574 20. doi:10.1080/14680629.2016.1201522.
27
28
29 575 [5] R. Rahbar-Rastega, R. Zhang, J.E. Sias, E. V. Dave, Evaluation of laboratory ageing
30
31 576 procedures on cracking performance of asphalt mixtures, *Road Mater. Pavement Des.*
32 577 0 (2019) 1–16. doi:10.1080/14680629.2019.1633782.
33
34
35 578 [6] Y. Zhang, T. Ma, X. Luo, X. Huang, R.L. Lytton, Prediction of Dynamic Shear
36
37 579 Modulus of Fine Aggregate Matrix Using Discrete Element Method and Modified
38
39 580 Hirsch Model, Elsevier Ltd, 2019. doi:10.1016/j.mechmat.2019.103148.
40
41 581 [7] Z. Zhou, X. Gu, Q. Dong, F. Ni, Y. Jiang, Low- and intermediate-temperature
42
43 582 behaviour of polymer-modified asphalt binders, mastics, fine aggregate matrices, and
44
45 583 mixtures with Reclaimed Asphalt Pavement material, *Road Mater. Pavement Des.* 0
46
47 584 (2019) 1–30. doi:10.1080/14680629.2019.1574233.
48
49
50 585 [8] X. Chen, M. Solaimanian, Simple Indexes to Identify Fatigue Performance of Asphalt
51
52 586 Concrete, *J. Test. Eval.* 48 (2020) 20170722. doi:10.1520/JTE20170722.
53
54 587 [9] M. Elwardany, F.Y. Rad, C. Castorena, Climate- , Depth- , and Time-Based
55
56 588 Laboratory Aging Procedure for Asphalt Mixtures, *Journal of the Association of*
57
58 589 *Asphalt Paving Technologists (AAPT)*, 87 (2018).
59
60
61
62
63
64
65

- 590 [10] M.D. Elwardany, F.Y. Rad, C. Castorena, Y.R. Kim, Evaluation of asphalt mixture
1 laboratory long-term aging methods for performance testing and prediction, *Asph.*
2 *Paving Technol. Sess.* 85 (2016) 35–75. doi:10.1080/14680629.2015.1266740.
3
4
5
6 593 [11] W.S. Mogawer, E.H. Fini, A.J. Austerman, Performance characteristics of high
7 reclaimed asphalt pavement containing bio-modifier, *Road Mater. Pavement Des.* 0629
8 (2016) 753–767. doi:10.1080/14680629.2015.1096820.
9
10 595
11
12 596 [12] A. Hanz, E. Dukatz, G. Reinke, Use of performance based testing for high RAP mix
13 design and production monitoring, *Asph. Paving Technol. Sess.* 85 (2016) 449–483.
14 597 doi:10.1080/14680629.2015.1266766.
15 598
16
17
18 599 [13] F. Yin, F. Kaseer, E. Arámbula-Mercado, A. Epps Martin, Characterising the long-
20 term rejuvenating effectiveness of recycling agents on asphalt blends and mixtures
21 with high RAP and RAS contents, *Road Mater. Pavement Des.* 18 (2017) 273–292.
22 601 doi:10.1080/14680629.2017.1389074.
23 602
24
25
26 603 [14] C. Chen, F. Yin, P. Turner, R.C. West, N. Tran, Selecting a Laboratory Loose Mix
27 Aging Protocol for the NCAT Top-Down Cracking Experiment, *Transp. Res. Rec.*
28 (2018) 1–13. doi:10.1177/0361198118790639.
29 604
30
31 605
32
33 606 [15] M. Nobakht, M.S. Sakhaeifar, Dynamic modulus and phase angle prediction of
34 laboratory aged asphalt mixtures, *Constr. Build. Mater.* 190 (2018) 740–751.
35 607 doi:10.1016/j.conbuildmat.2018.09.160.
36 608
37
38
39 609 [16] H. Sahebzamani, M.Z. Alavi, O. Farzaneh, Evaluating effectiveness of polymerized
41 pellets mix additives on improving asphalt mix properties, *Constr. Build. Mater.* 187
42 610 (2018) 160–167. doi:10.1016/j.conbuildmat.2018.07.143.
43 611
44
45
46 612 [17] R. Rahbar-Rastegar, J.S. Daniel, E. V. Dave, Evaluation of Viscoelastic and Fracture
47 Properties of Asphalt Mixtures with Long-Term Laboratory Conditioning, *Transp.*
48 613 *Res. Rec.* (2018). doi:10.1177/0361198118795012.
49 614
50
51
52 615 [18] C. Ogbo, F. Kaseer, M. Oshone, J.E. Sias, A.E. Martin, Mixture-based rheological
53 616 evaluation tool for cracking in asphalt pavements, *Road Mater. Pavement Des.* 5
54 (2019) 1–16. doi:10.1080/14680629.2019.1592010.
55 617
56
57
58 618 [19] Y.-R. Kim, D. Little, I. Song, Effect of Mineral Fillers on Fatigue Resistance and
59
60
61
62
63
64
65

- 619 Fundamental Material Characteristics: Mechanistic Evaluation, *Transp. Res. Rec. J.*
1
2 620 *Transp. Res. Board.* 1832 (2003) 1–8. doi:10.3141/1832-01.
3
- 4 621 [20] S.N. Suresha, A. Ningappa, Recent trends and laboratory performance studies on FAM
5 mixtures : A state-of-the-art review, *Constr. Build. Mater.* 174 (2018) 496–506.
6 622 doi:10.1016/j.conbuildmat.2018.04.144.
7
- 8 623
9
- 10 624 [21] Y.-R. Kim, D.N. Little, R.L. Lytton, Fatigue and Healing Characterization of Asphalt
11 Mixtures, *J. Mater. Civ. Eng.* 15 (2003) 75–83. doi:10.1061/(ASCE)0899-
12 625 1561(2003)15:1(75).
13
14 626
- 15
16
- 17 627 [22] E. Masad, V.T.F. Castelo Branco, D.N. Little, R. Lytton, A unified method for the
18 analysis of controlled-strain and controlled-stress fatigue testing, *Int. J. Pavement Eng.*
19 628 9 (2008) 233–246. doi:10.1080/10298430701551219.
20
21 629
- 22
- 23 630 [23] S. Caro, E. Masad, G. Airey, A. Bhasin, D. Little, Probabilistic Analysis of Fracture in
24 Asphalt Mixtures Caused by Moisture Damage, *Transp. Res. Rec. J. Transp. Res.*
25 631 *Board.* 2057 (2008) 28–36. doi:10.3141/2057-04.
26
27 632
- 28
29
- 30 633 [24] V. Castelo Branco, E. Masad, A. Bhasin, D. Little, Fatigue Analysis of Asphalt
31 Mixtures Independent of Mode of Loading, *Transp. Res. Rec. J. Transp. Res. Board.*
32 634 2057 (2008) 149–156. doi:10.3141/2057-18.
33
34 635
- 35
- 36 636 [25] P. Karki, R. Li, A. Bhasin, Quantifying overall damage and healing behaviour of
37 asphalt materials using continuum damage approach, *Int. J. Pavement Eng.* 16 (2015)
38 637 350–362. doi:10.1080/10298436.2014.942993.
39
40 638
- 41
- 42 639 [26] S. Im, T. You, H. Ban, Y.R. Kim, Multiscale testing-analysis of asphaltic materials
43 considering viscoelastic and viscoplastic deformation, *Int. J. Pavement Eng.* 18 (2017)
44 640 783–797. doi:10.1080/10298436.2015.1066002.
45
46 641
- 47
48
- 49 642 [27] F.T.S. Aragão, Y.R. Kim, Mode I Fracture Characterization of Bituminous Paving
50 Mixtures at Intermediate Service Temperatures, *Exp. Mech.* 52 (2012) 1423–1434.
51 643 doi:10.1007/s11340-012-9594-4.
52
53 644
- 54
- 55 645 [28] B.S. Underwood, Y.R. Kim, Effect of volumetric factors on the mechanical behavior
56 of asphalt fine aggregate matrix and the relationship to asphalt mixture properties,
57 646 *Constr. Build. Mater.* 49 (2013) 672–681. doi:10.1016/j.conbuildmat.2013.08.045.
58
59 647
- 60
61
62
63
64
65

- 648 [29] B.S. Underwood, Y.R. Kim, Experimental investigation into the multiscale behaviour
649 of asphalt concrete, *Int. J. Pavement Eng.* 12 (2011) 357–370.
650 doi:10.1080/10298436.2011.574136.
- 651 [30] K. Bemis, K. Bennett, Using numerical models and volume rendering to interpret
652 acoustic imaging of hydrothermal flow, *EOS Trans. Am. Geophys. Union.* 25 (2009)
653 1209–1219. doi:10.1061/(ASCE)MT.1943-5533.0000673.
- 654 [31] T. Report, D. Page, P. Covered, Fracture Properties and Fatigue Cracking Resistance
655 of Asphalt Binders March 2012 Arash Motamed , Amit Bhasin , and Anoosha Izadi
656 Report 161122-1 Center for Transportation Research University of Texas at Austin
657 1616 Guadalupe Street , Suite 4 . 200 Southw, 7 (2012).
- 658 [32] J. Zhu, M.Z. Alavi, J. Harvey, L. Sun, Y. He, Evaluating fatigue performance of fine
659 aggregate matrix of asphalt mix containing recycled asphalt shingles, *Constr. Build.*
660 *Mater.* 139 (2017) 203–211. doi:10.1016/j.conbuildmat.2017.02.060.
- 661 [33] C. Chen, F. Yin, P. Turner, R.C. West, N. Tran, Selecting a Laboratory Loose Mix
662 Aging Protocol for the NCAT Top-Down Cracking Experiment, *Transp. Res. Rec.*
663 (2018). doi:10.1177/0361198118790639.
- 664 [34] Hanz, Andrew Dukatz, Ervin Reinke, Gerald Use of performance based testing for
665 high RAP mix design and production monitoring, *Road Mater. Pavement Des.* 18(1),
666 (2016), 284-310. DOI: 10.1080/14680629.2016.1266766.
- 667 [35] Y. He, M.Z. Alavi, D. Jones, J. Harvey, Proposing a solvent-free approach to evaluate
668 the properties of blended binders in asphalt mixes containing high quantities of
669 reclaimed asphalt pavement and recycled asphalt shingles, *Constr. Build. Mater.* 114
670 (2016) 172–180. doi:10.1016/j.conbuildmat.2016.03.074.
- 671 [36] V. Branco, A. Bhasin, E. Masad, D. Little, J. Soares, Separation of Nonlinear
672 Viscoelastic Response From Fatigue Damage Using Dynamic Mechanical Analysis
673 (Dma), (2008) 1–13.
- 674 [37] P. Sousa, E. Kassem, E. Masad, D. Little, New design method of fine aggregates
675 mixtures and automated method for analysis of dynamic mechanical characterization
676 data, *Constr. Build. Mater.* 41 (2013) 216–223.
677 doi:10.1016/j.conbuildmat.2012.11.038.

- 678 [38] R.A. Freire, L. F. A. L. Babadopulos, V. T. F. Castelo Branco, A. Bhasin, Aggregate
1 Maximum Nominal Sizes' Influence on Fatigue Damage Performance Using Different
2 Scales, *J. Mater. Civ. Eng.* 29 (2017) 04017067. doi:10.1061/(ASCE)MT.1943-
3 5533.0001912.
4
5
6
7
8 [39] Q. Li, Fatigue resistance investigation of warm mix recycled asphalt binder, mastic,
9 and fine aggregate matrix, *Wiley*. 31 (2017) 233–248. doi:10.1111/ffe.12692.
10
11
12 [40] A.K.Y. Ng, A.C. Vale, A.C. Gigante, A.L. Faxina, D. Ph, Determination of the Binder
13 Content of Fine Aggregate Matrices Prepared with Modified Binders, *J. Mater. Civ.*
14 *Eng. ASCE*. 30 (2018) 1–12. doi:10.1061/(ASCE)MT.1943-5533.0002160.
15
16
17
18 [41] ANDRISE BUCHWEITZ KLUG ABK, Evaluation of the fatigue performance of fine
19 aggregate matrices prepared with reclaimed asphalt pavements and shale oil residue,
20 2017. doi:10.11606/D.18.2018.tde-19022018-112755.
21
22
23
24
25 [42] M. Sadeq, H. Al-Khalid, E. Masad, O. Sirin, Comparative evaluation of fatigue
26 resistance of warm fine aggregate asphalt mixtures, *Constr. Build. Mater.* 109 (2016)
27 8–16. doi:10.1016/j.conbuildmat.2016.01.045.
28
29
30
31 [43] Q. Li, G. Li, X. Ma, S. Zhang, Linear viscoelastic properties of warm-mix recycled
32 asphalt binder, mastic, and fine aggregate matrix under different aging levels, *Constr.*
33 *Build. Mater.* 192 (2018) 99–109. doi:10.1016/j.conbuildmat.2018.10.085.
34
35
36
37 [44] Y.-R. Kim, D.N. Little, R.L. Lytton, Evaluation of microdamage, healing, and heat
38 dissipation of asphalt mixtures, using a dynamic mechanical analyzer, *Transp. Res.*
39 *Rec.* (2001) 60–66. doi:10.3141/1767-08.
40
41
42
43 [45] S. Caro, D.B. Sánchez, B. Caicedo, Methodology to characterise non-standard asphalt
44 materials using DMA testing: Application to natural asphalt mixtures, *Int. J. Pavement*
45 *Eng.* 16 (2015) 1–10. doi:10.1080/10298436.2014.893328.
46
47
48
49 [46] F.T.S. Aragão, J. Lee, Y.R. Kim, P. Karki, Material-specific effects of hydrated lime
50 on the properties and performance behavior of asphalt mixtures and asphaltic
51 pavements, *Constr. Build. Mater.* 24 (2010) 538–544.
52
53
54
55
56
57
58 [47] H. Nabizadeh, H.F. Haghshenas, Y.R. Kim, F.T.S. Aragão, Effects of rejuvenators on
59
60
61
62
63
64
65

- 707 high-RAP mixtures based on laboratory tests of asphalt concrete (AC) mixtures and
1 708 fine aggregate matrix (FAM) mixtures, *Constr. Build. Mater.* 152 (2017) 65–73.
2
3 709 doi:10.1016/j.conbuildmat.2017.06.101.
4
5
6 710 [48] M.O. Marasteanu, D.A. Anderson, Establishing Linear Viscoelastic Conditions for
7
8 711 Asphalt Binders, *Transp. Res. Rec. J. Transp. Res. Board.* (2007). doi:10.3141/1728-
9
10 712 01.
11
12 713 [49] D.B. Sánchez, G. Airey, S. Caro, J. Grenfell, Effect of foaming technique and mixing
13
14 714 temperature on the rheological characteristics of fine RAP-foamed bitumen mixtures,
15
16 715 *Road Mater. Pavement Des.* 0 (2019) 1–17. doi:10.1080/14680629.2019.1593228.
17
18
19 716 [50] N.I.M. Yusoff, F.M. Jakarni, V.H. Nguyen, M.R. Hainin, G.D. Airey, Modelling the
20
21 717 rheological properties of bituminous binders using mathematical equations, *Constr.*
22
23 718 *Build. Mater.* 40 (2013) 174–188. doi:10.1016/j.conbuildmat.2012.09.105.
24
25 719 [51] S. Yang, A. Braham, S. Underwood, A. Hanz, G. Reinke, Correlating field
26
27 720 performance to laboratory dynamic modulus from indirect tension and torsion bar,
28
29 721 *Asph. Paving Technol. Assoc. Asph. Paving Technol. Tech. Sess.* 85 (2016) 131–162.
30
31 722 doi:10.1080/14680629.2015.1267438.
32
33 723 [52] R. Nemati, E. V Dave, Nominal property based predictive models for asphalt mixture
34
35 724 complex modulus (dynamic modulus and phase angle), 158 (2018) 308–319.
36
37 725 doi:10.1016/j.conbuildmat.2017.09.144.
38
39
40 726 [53] R. Rahbar-rastegar, CRACKING IN ASPHALT PAVEMENTS : IMPACT OF
41
42 727 COMPONENT PROPERTIES AND AGING ON FATIGUE AND THERMAL
43
44 728 CRACKING, (2017). Doctoral Dissertations. 2284.
45
46 729 <https://scholars.unh.edu/dissertation/2284>
47
48 730 [54] R. Nemati, Evaluation of Structural Contribution of Asphalt Mixtures Through
49
50 731 Improved Performance Indices, (2019). Doctoral Dissertations. 2460.
51
52 732 <https://scholars.unh.edu/dissertation/2460>
53
54 733 [55] D.B. Sánchez, J. Grenfell, G. Airey, S. Caro, Evaluation of the degradation of fine
55
56 734 asphalt-aggregate mixtures containing high reclaimed asphalt pavement contents, *Road*
57
58 735 *Mater. Pavement Des.* 18 (2017) 91–107. doi:10.1080/14680629.2017.1304250.
59
60
61
62
63
64
65

736 [56] H.F. Haghshenas, H. Nabizadeh, Y.-R. Kim, The Effect of Rejuvenators on RAP
1 737 Mixtures: A Study Based on Multiple Scale Laboratory Test Results, *Geo-Chicago*
2 738 2016. (2016) 697–707. doi:10.1061/9780784480137.066.
3
4
5
6 739 [57] Y. Kim, H. Lee, Evaluation of the effect of aging on mechanical and fatigue properties
7 of sand asphalt mixtures, *KSCE J. Civ. Eng.* 7 (2003) 389–398.
8 740 doi:10.1007/BF02895837.
9 741
10
11
12 742 [58] M.E. Kutay, N. Gibson, J. Youtcheff, Conventional and Viscoelastic Continuum
13 743 Damage (VECD) - Based Fatigue Analysis of Polymer Modified Asphalt Pavements,
14 744 *J. Assoc. Asph. Paving Technol.* (2008).
15
16
17
18
19 745 [59] B.J. Smith, S.A.. Hesp, Crack pinning in asphalt mastic and concrete, *Transp. Res.*
20 746 *Rec. J. Transp. Res. Board.* 1728 (2000) 75–81.
21
22
23 747 [60] P. Karki, A. Bhasin, B.S. Underwood, Fatigue Performance Prediction of Asphalt
24 748 Composites Subjected to Cyclic Loading with Intermittent Rest Periods, *Transp. Res.*
25 749 *Rec. J. Transp. Res. Board.* 2576 (2016) 72–82. doi:10.3141/2576-08.
26
27
28
29
30 750 [61] H. Nabizadeh, Viscoelastic, Fatigue Damage, and Permanent Deformation
31 751 Characterization of High Rap Bituminous Mixtures Using Fine Aggregate Matrix
32 752 (Fam), (2015) 88.
33 753 <http://digitalcommons.unl.edu/civilengdiss%5Cnhttp://digitalcommons.unl.edu/civilen>
34 754 [gdiss.](http://digitalcommons.unl.edu/civilen)
35
36
37
38
39
40 755 [62] Sanchez, Meso-scale Rheological Characteristics of Foamed Bitumen Mixtures with
41 756 High RAP Content (2018).
42 757 <http://eprints.nottingham.ac.uk/50503/1/Final%20PhD%20Thesis%20Diana%20March>
43 758 [%202018%20after%20viva.pdf](http://eprints.nottingham.ac.uk/50503/1/Final%20PhD%20Thesis%20Diana%20March)
44
45
46
47
48 759 [63] D.J. Mensching, A. Andriescu, C. Decarlo, X. Li, J.S. Youtcheff, Effect of Extended
49 760 Aging on Asphalt Materials Containing Rerefined Engine Oil Bottoms, *Transp. Res.*
50 761 *Board TRB 2017 Annu. Meet.* (2017) 1–18.
51
52
53
54 762 [64] D. Singh, M. Zaman, S. Commuri, Evaluation of predictive models for estimating
55 763 dynamic modulus of hot-mix asphalt in Oklahoma, *Transp. Res. Rec.* (2011) 57–72.
56 764 doi:10.3141/2210-07.
57
58
59
60
61
62
63
64
65

1
2 765 [65] W.R. Kingery, Laboratory Study of Fatigue Characteristics of HMA Surface Mixtures
3 Containing Recycled Asphalt Pavement (RAP), (2004).
4
5 767 [66] K. Aravind, A. Das, Pavement design with central plant hot-mix recycled asphalt
6 mixes, Constr. Build. Mater. 21 (2007) 928–936.
7
8 769 doi:10.1016/j.conbuildmat.2006.05.004.
9
10 770
11
12 771
13
14 772
15
16
17
18
19
20
21
22
23
24
25
26
27
28
29
30
31
32
33
34
35
36
37
38
39
40
41
42
43
44
45
46
47
48
49
50
51
52
53
54
55
56
57
58
59
60
61
62
63
64
65

Table 1. Basic properties of asphalt binder

Property	Test Results	Limiting value IS 73:2013
Penetration at 25°C, 0.1 mm	64.5	Min. 45
Softening point (R&B) (°C)	52.7	45-55
Ductility at 25°C (cm)	85.4	Min. 70
Absolute viscosity at 60°C (poise)	2700	2400-3600
Kinematic viscosity at 135°C (cSt)	438	Min. 350
Flash Point (°C)	≥220	Min. 220

Table 2. Details of method to fabricate FAM specimens

Steps	STA/LTA	Temperature	Time
Pre-heating of fine aggregates and asphalt binder		153°C	40 min
Mixing of loose FAM mixture			
Loose FAM mixture	STA	135°C	4 hrs
Loose FAM mixture	LTA	135°C	6, 12, and 24 hrs
Loose FAM mixture	LTA	95°C	5, and 12 days
Pre-heating of moulds		135°C	1 hr
Pre-heating		135°C	2 hrs
Compacting			
Compacted specimens	LTA	85°C	5 days
Cooling		AC room at 18°C	2 hrs
Extraction of specimens from the moulds			
Equilibration		Room temperature	24 hrs

Table 3. Details of Different FAM Combinations

Binder Type	Properties	Test Name	FAM Mixture Type							Number of Specimens
			Loose Mixture Aging						Compacted Specimen Aging	
			A	A1	A2	A3	B1	B2	C	
VG-30	Viscoelastic	Strain sweep	3	3	3	3	3	3	3	3x7=21
		Temp. and freq. sweep	3	3	3	3	3	3	3	3x7=21
	Fatigue	Time sweep @ 4 strain levels	3x4	3x4	3x4	3x4	3x4	3x4	3x4	3x4x7=84

Note: A=4 hrs at 135°C, A1=6 hrs at 135°C, A2=12 hrs at 135°C, A3=24 hrs at 135°C, B1=5 days at 95°C, B2=12 days at 95°C, C=5 days at 85°C, VG=Viscosity grade

Table 4. Complex shear modulus $|G^*|$ master curve parameters of FAM mixtures

Mixture Type	α	β	γ	κ
A	7.04	2.73	-0.15	-0.55
A1	6.78	3.47	-0.33	-0.31
A2	6.79	3.58	-0.43	-0.28
A3	7.32	2.65	-0.56	-0.30
C	6.97	3.19	-0.22	-0.40
B1	6.84	3.35	-0.35	-0.36
B2	6.33	4.23	-0.57	-0.22

Table 5. Slope between each FAM mixtures at different frequency levels

Mixture Type	Slope, m		
	At lower reduced frequency (0.00005 rad/s)	At intermediate reduced frequency (1.5 rad/s)	At higher reduced frequency (5250 rad/s)
A	0.018	0.069	0.170
A1	0.394	0.158	0.190
A2	0.678	0.197	0.222
A3	1.202	0.167	0.078
C	0.187	0.158	0.297
B1	0.275	0.177	0.240
B2	1.323	0.217	0.205

Table 6. Phase angle master curve parameters of FAM mixtures

Mixture Type	a	b	c
A	35.02	-4.36	-0.07
A1	27.04	-7.91	-1.74
A2	24.44	-10.05	-2.68
A3	20.21	-13.64	-5.77
C	30.42	-6.08	-0.73
B1	28.81	-6.88	-1.50
B2	24.52	-14.01	-5.95

Table 7. Goodness-of-fit results of $|G^*|$ and δ from master curve analysis

Mixture Type	$ G^* , R^2$	Acceptance criteria, [50,64]	δ, R^2	Acceptance criteria, [50,64]
	Coefficient of determination	Coefficient of determination	Coefficient of determination	Coefficient of determination
A	0.997	Excellent (≥ 0.90)	0.87	Good (0.70-0.89)
A1	0.990	Excellent (≥ 0.90)	0.71	Good (0.70-0.89)
A2	0.827	Good (0.70-0.89)	0.71	Good (0.70-0.89)
A3	0.900	Excellent (≥ 0.90)	0.93	Excellent (≥ 0.90)
C	0.975	Excellent (≥ 0.90)	0.73	Good (0.70-0.89)
B1	0.974	Excellent (≥ 0.90)	0.70	Good (0.70-0.89)
B2	0.990	Excellent (≥ 0.90)	0.84	Good (0.70-0.89)

Table 8. Fatigue model regression coefficients

Mixture type	Fatigue model regression coefficients	
	a	b
A	430.790	-1.934
A1	679.020	-1.840
A2	71.845	-2.627
A3	27.406	-2.861
C	924.390	-1.553
B1	708.080	-1.689
B2	283.650	-1.815

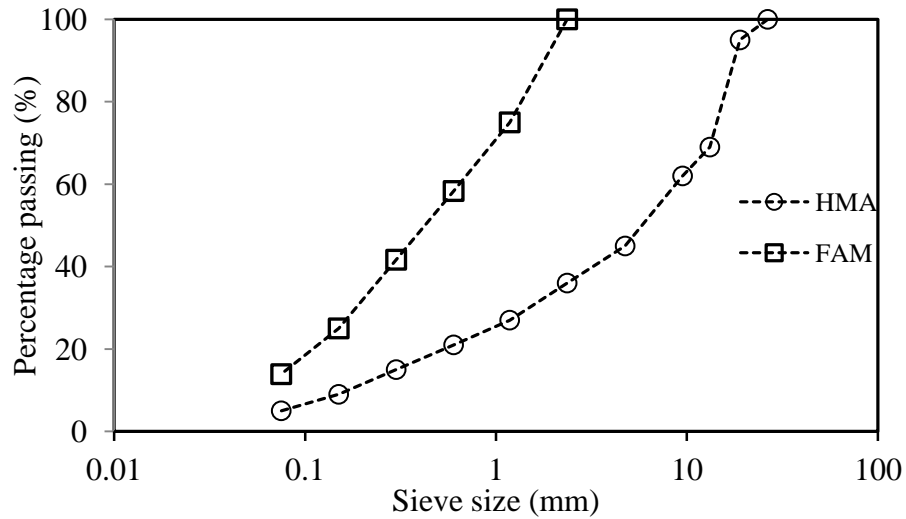


Fig. 1. Aggregate gradation for HMA and FAM mix design

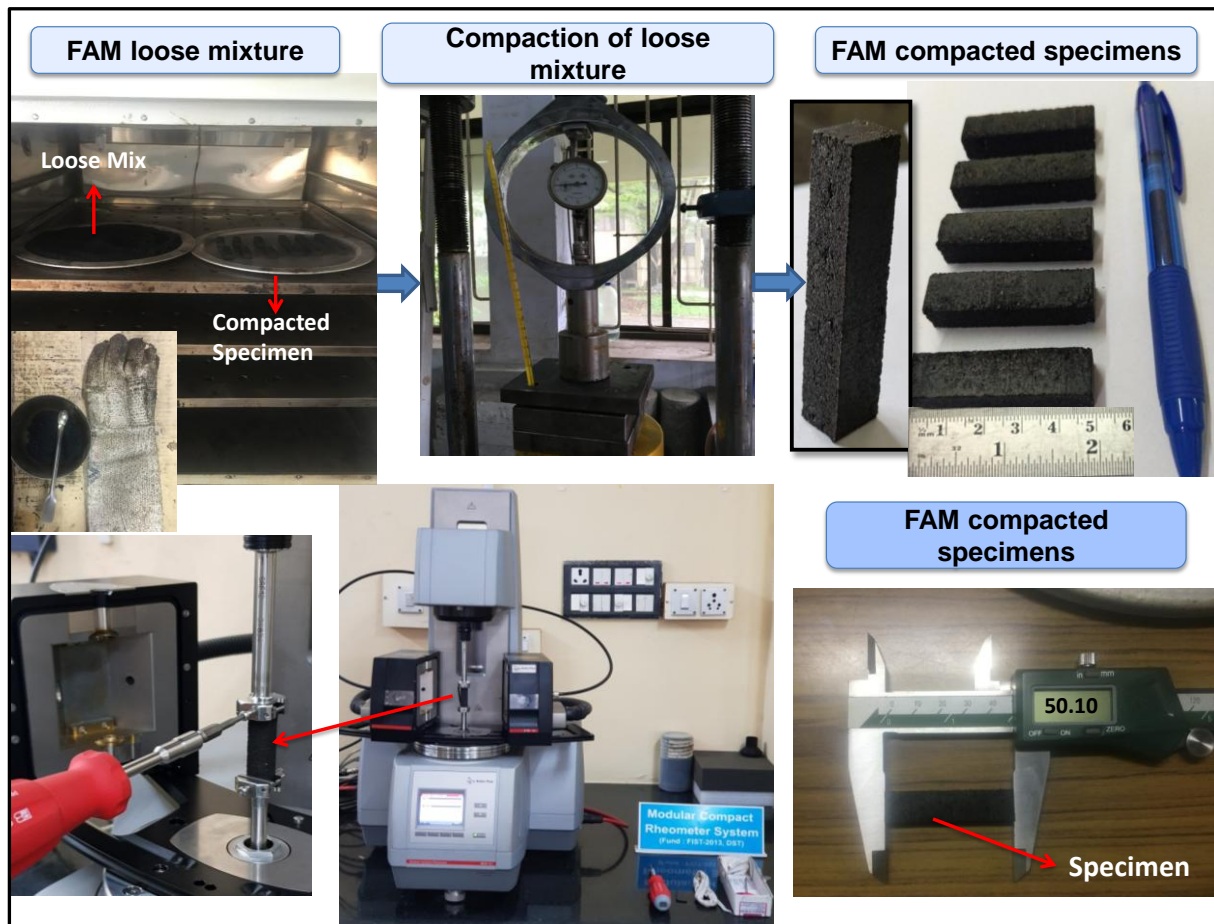


Fig. 2. Rectangular FAM Specimen Preparation



Fig. 3. Dynamic Shear Rheometer (MCR 502) Setup.

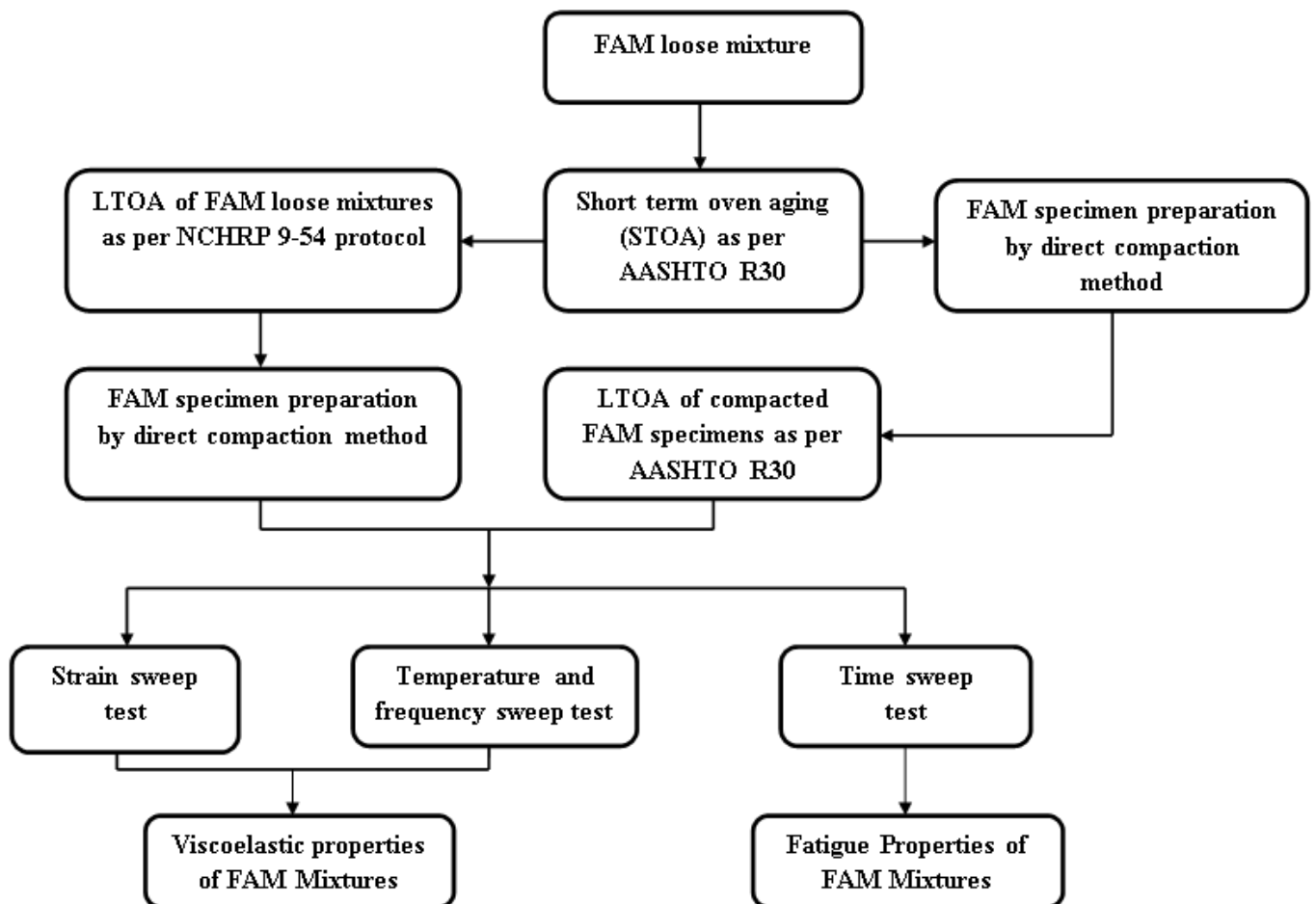


Fig. 4. Overall experimental plan

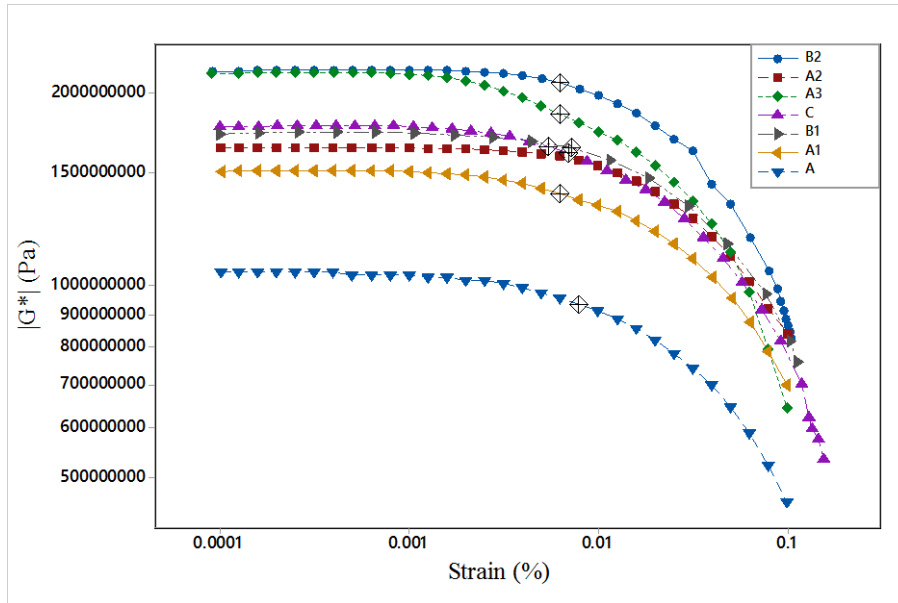


Fig. 5. Results of FAM strain sweep test

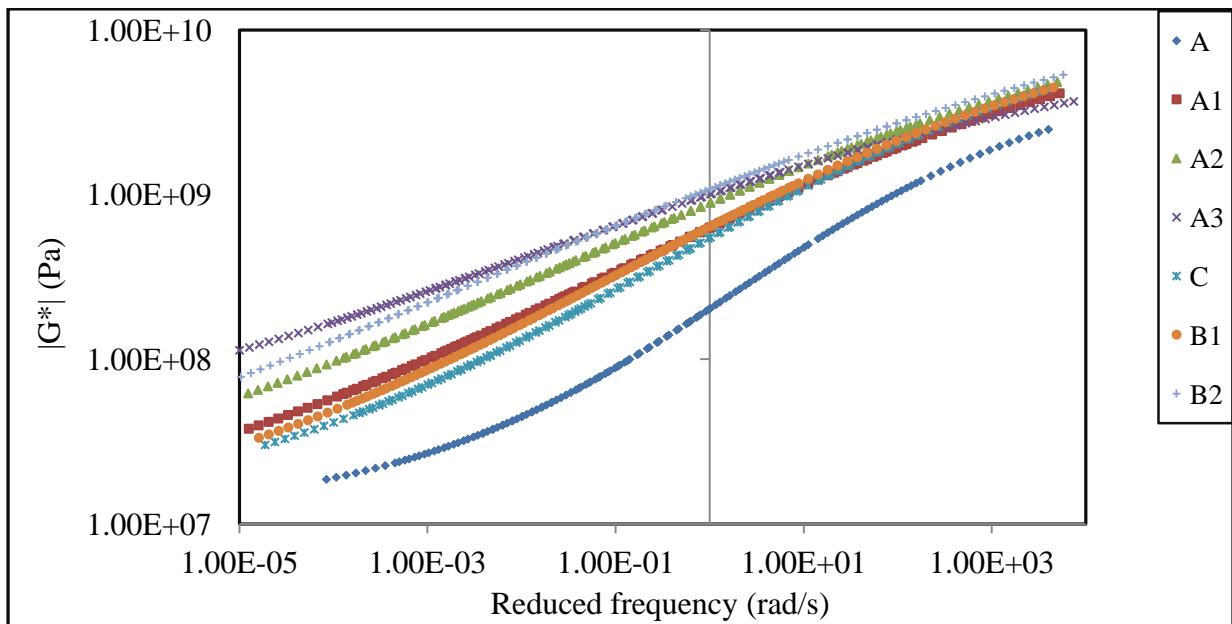


Fig. 6. Complex shear modulus $|G^*|$ of STOA and LTOA FAM mixtures at reference temperature 25°C.

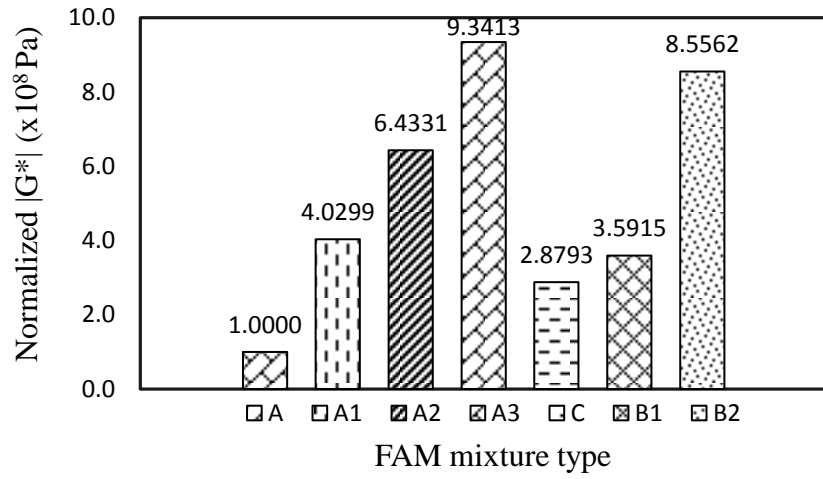


Fig. 7. Normalised $|G^*|$ of FAM mixtures at 0.001Hz and 25°C.

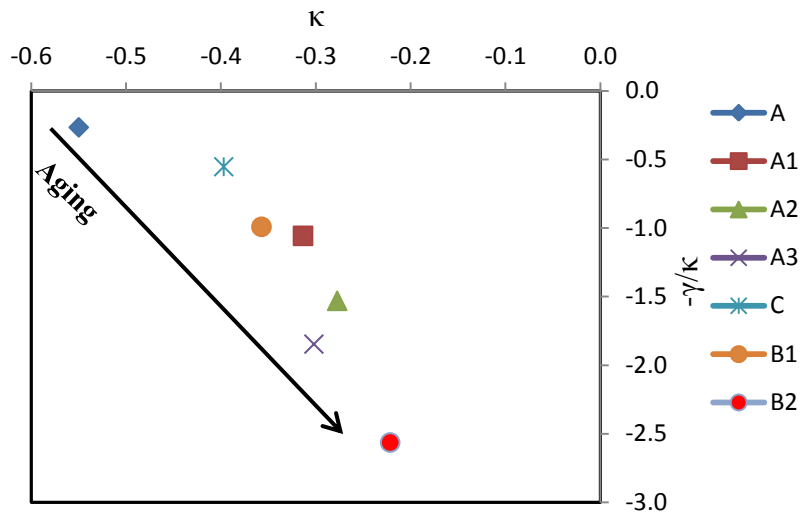


Fig. 8. Variations of $|G^*|$ master curve shape parameter with different aging levels at a reference temperature of 25°C.

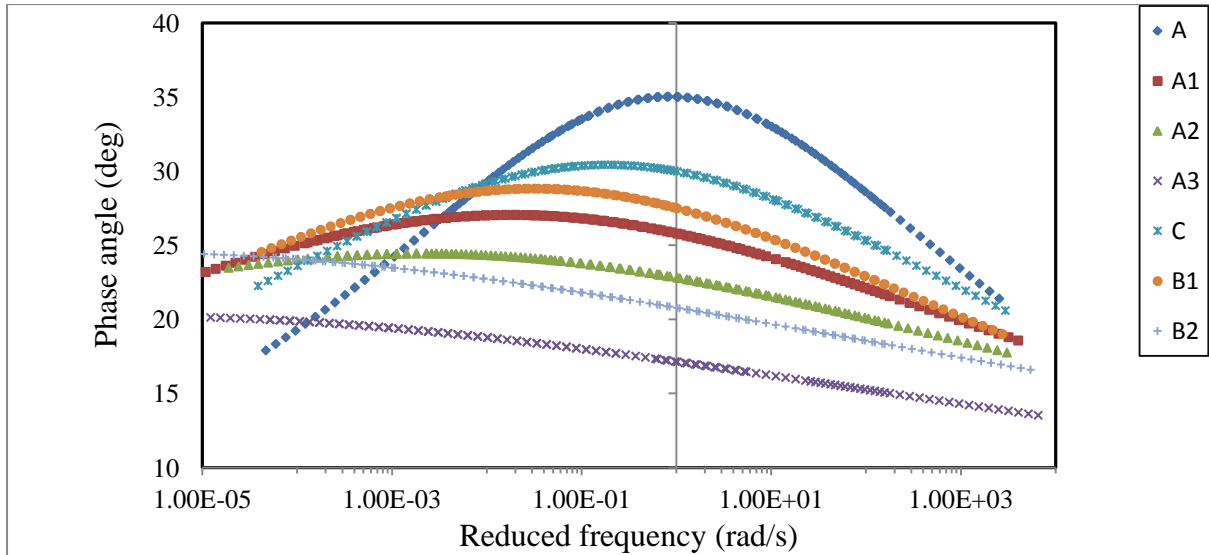


Fig. 9. Phase angle of STA and LTA FAM mixtures at a reference temperature of 25°C.

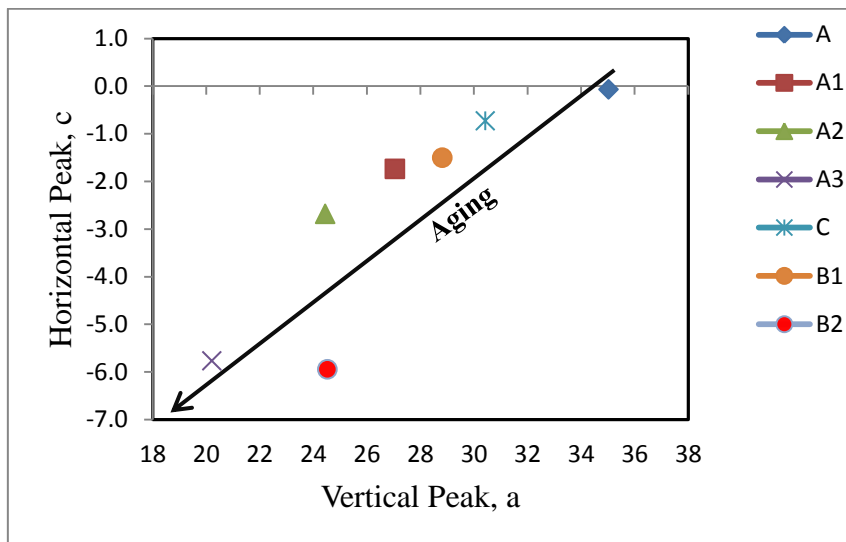


Fig. 10. Variations of δ master curve shape parameter with different aging levels at a reference temperature of 25°C.

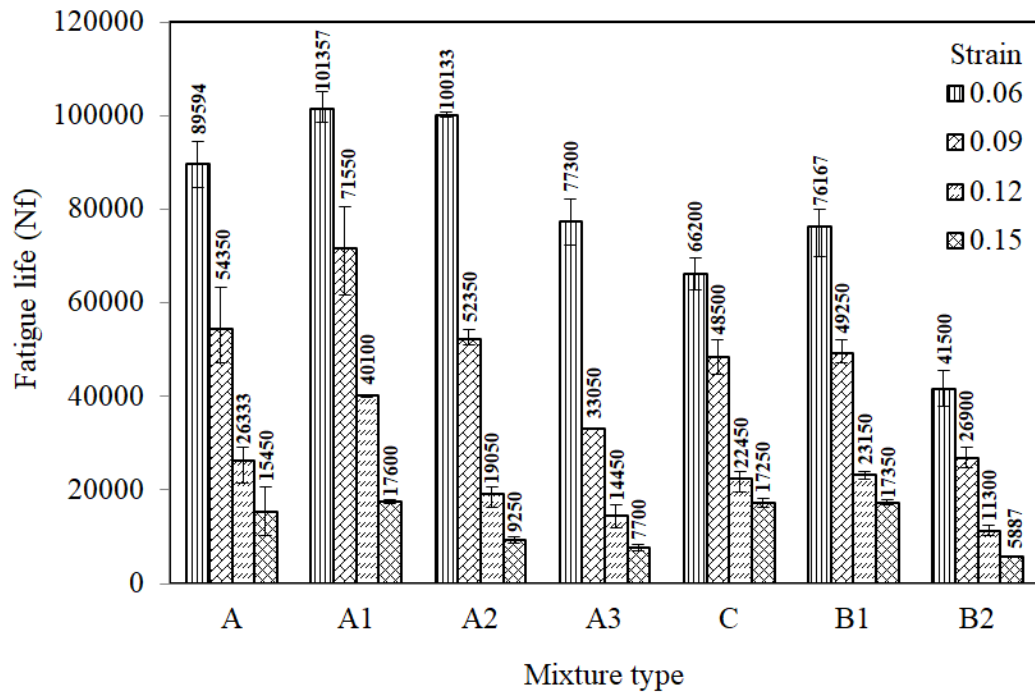


Fig. 11. Strain controlled fatigue test results at 25°C and the frequency of 10Hz

***Declaration of Interest Statement**

None.